



UNIVERSITY OF LEEDS

This is a repository copy of *Calibration of the oxygen and clumped isotope thermometers for (proto-)dolomite based on synthetic and natural carbonates*.

White Rose Research Online URL for this paper:  
<http://eprints.whiterose.ac.uk/151982/>

Version: Accepted Version

---

**Article:**

Müller, IA, Rodriguez-Blanco, JD, Storck, JC et al. (5 more authors) (2019) Calibration of the oxygen and clumped isotope thermometers for (proto-)dolomite based on synthetic and natural carbonates. *Chemical Geology*, 525. pp. 1-17. ISSN 0009-2541

<https://doi.org/10.1016/j.chemgeo.2019.07.014>

---

© 2019, Elsevier. This manuscript version is made available under the CC-BY-NC-ND 4.0 license <http://creativecommons.org/licenses/by-nc-nd/4.0/>.

**Reuse**

This article is distributed under the terms of the Creative Commons Attribution-NonCommercial-NoDerivs (CC BY-NC-ND) licence. This licence only allows you to download this work and share it with others as long as you credit the authors, but you can't change the article in any way or use it commercially. More information and the full terms of the licence here: <https://creativecommons.org/licenses/>

**Takedown**

If you consider content in White Rose Research Online to be in breach of UK law, please notify us by emailing [eprints@whiterose.ac.uk](mailto:eprints@whiterose.ac.uk) including the URL of the record and the reason for the withdrawal request.



[eprints@whiterose.ac.uk](mailto:eprints@whiterose.ac.uk)  
<https://eprints.whiterose.ac.uk/>

1 Calibration of the oxygen and clumped isotope thermometers for dolomite based on synthetic and  
2 natural carbonates.

3

4 Inigo A. Müller<sup>1,2</sup>, Juan D. Rodriguez-Blanco<sup>3,5</sup>, Julian-Christopher Storck<sup>2</sup>, Gabriela Santilli do  
5 Nascimento<sup>2</sup>, Crisogono Vasconcelos<sup>2</sup>, Liane G. Benning<sup>4,5,6</sup>, Stefano M. Bernasconi<sup>2</sup>

6

7 <sup>1</sup>Faculty of Geosciences, Utrecht University, Utrecht, Netherlands

8 <sup>2</sup>Department of Earth Sciences, ETH Zurich, Zurich, Switzerland

9 <sup>3</sup>iCRAG Department of Geology, School of Natural Sciences, Trinity College Dublin, Dublin, Ireland

10 <sup>4</sup>German Research Centre for Geosciences, GFZ, Potsdam, Germany

11 <sup>5</sup>School of Earth and Environment, University of Leeds, Leeds, UK

12 <sup>6</sup>Department of Geology, Free University of Berlin, Berlin, Germany

13

14

15

1  
2  
3  
4  
5  
6  
7  
8  
9  
10  
11  
12  
13  
14  
15  
16  
17  
18  
19  
20  
21  
22  
23  
24  
25  
26  
27  
28  
29  
30  
31  
32  
33  
34  
35  
36  
37  
38  
39  
40  
41  
42  
43  
44  
45  
46  
47  
48  
49  
50  
51  
52  
53  
54  
55  
56  
57  
58  
59  
60  
61  
62  
63  
64  
65

## 16 Abstract

17 Dolomite is a very common carbonate mineral in ancient sediments, but is rarely found in modern  
18 environments. Because of the difficulties in precipitating dolomite in the laboratory at low  
19 temperatures, the controls on its formation are still debated after more than two centuries of  
20 research. Two important parameters to constrain the environment of dolomitization are the  
21 temperature of formation and the oxygen isotope composition of the fluid from which it  
22 precipitated. Carbonate clumped isotopes (expressed with the parameter  $\Delta_{47}$ ) are increasingly  
23 becoming the method of choice to obtain this information. However, whereas many clumped isotope  
24 studies treated dolomites the same way as calcite, some recent studies observed a different  
25 phosphoric acid fractionation for  $\Delta_{47}$  during acid digestion of dolomite compared to calcite. This  
26 causes additional uncertainties in the  $\Delta_{47}$  temperature estimates for dolomites analyzed in different  
27 laboratories using different acid digestion temperatures.

28 To solve this problem we present here a dolomite-specific  $\Delta_{47}$ -temperature calibration from 25 to  
29 1100 °C with acid reaction temperature of 70 °C and anchored to widely available carbonate  
30 standards. For the temperature range 25 to 220 °C we obtain a linear  $\Delta_{47}$ -T relationship:

$$31 \Delta_{47 \text{ CDES } 70^\circ \text{ C}} = 0.0426 \pm 0.0022 \times \left(\frac{10^6}{T^2}\right) + 0.1492 \pm 0.0169 \quad (T = \text{temperature in Kelvin})$$

32 Including two isotopically scrambled dolomites formed at 1100 °C the best fit is obtained with a third  
33 order polynomial temperature relationship of

$$34 \Delta_{47 \text{ CDES } 70^\circ \text{ C}} (\text{‰}) = -0.0002 \times \left(\frac{10^6}{T^2}\right)^3 + 0.0042 \times \left(\frac{10^6}{T^2}\right)^2 + 0.0113 \times \left(\frac{10^6}{T^2}\right) + 0.2219.$$

35 Applying a calcite  $\Delta_{47}$ -T relationship results in 10 to 16 °C colder formation temperatures for  
36 dolomites than using the dolomite specific calibration presented here.

37 For the synthetic samples formed between 70 and 220 °C we also determined the temperature  
38 dependence of the oxygen isotope fractionation relative to the water. Based on the similarity  
39 between our results and two other recent studies we propose that a combination of the three  
40 datasets represents the most robust calibration for dolomite formed in a wide temperature range  
41 from 25 to 350 °C.

$$54 10^3 \alpha_{\text{Dolomite-Water}} = 2.9923 \pm 0.0557 \times \left(\frac{10^6}{T^2}\right) - 2.3592 \pm 0.4116$$

42 Because of the uncertainties in the phosphoric acid oxygen and clumped isotope fractionation for  
43 dolomite, we introduce three samples that are available in large amounts as possible inter-laboratory  
44 calibration standard for oxygen and clumped isotope measurements. A sample of the middle Triassic

45 San Salvatore dolomite from southern Switzerland, the NIST SRM 88b dolomite standard and a  
46 lacustrine Pliocene dolomite from La Roda (Spain).

47 This study demonstrates the necessity to apply dolomite specific  $\Delta_{47}$ -T relationships for accurate  
48 temperature estimates of dolomite formation, ideally done at identical acid digestion temperatures  
49 to avoid acid digestion temperature corrections. In addition, the simultaneous analyses of dolomite  
50 standards will enable a much better comparison of published dolomite clumped and oxygen isotope  
51 data amongst different laboratories.

52

## 53 1. INTRODUCTION

54 The formation of dolomite ( $\text{Ca,Mg}(\text{CO}_3)_2$ ) in nature has been subject to extensive research for more  
55 than two centuries. In spite of all the efforts it remains unclear how this mineral forms at Earth  
56 surface conditions and why it is so abundant during certain time intervals in the geological past  
57 (Land, 1985; Given and Wilkinson, 1987; Spencer and Hardie, 1990; Chai et al., 1995; Hardie, 1996;  
58 Holland et al., 1996; Wright, 1997; Land, 1998; Burns et al., 2000; Warren, 2000). In modern  
59 environments only few places of active (proto-)dolomite formation at the surface are known and in  
60 most of these cases microorganisms have been shown to play an active or passive role (e.g.  
61 Vasconcelos and McKenzie, 1997; Wright, 1999; Bontognali et al., 2010; Brauchli et al., 2016).  
62 However, the amount and geographic extent of recent dolomite formation is only very small  
63 compared to the amounts that were formed during specific time intervals in the past, such as the  
64 Triassic (Berra et al., 2010) or the Cryogenian (Hood et al., 2011; Hood and Wallace, 2012). Such  
65 episodes of widespread dolomite formation were followed and preceded by time intervals where  
66 limestone ( $\text{CaCO}_3$ ) was the dominant carbonate sediment. These transitions between dolomite and  
67 limestone-rich time intervals in the geological record are thought to be triggered by changes in global  
68 seawater chemistry or by changes in the depositional environment (e.g. Hardie, 1996; Holland et al.,  
69 1996). To improve our models of dolomitization it is crucial to better characterize the temperature of  
70 formation and the composition of the fluid responsible for dolomite formation.

71 Many examples exist where microstructures and fossils in ancient dolomites point to a very early  
72 diagenetic formation in shallow seawater or lacustrine environment (e.g. Frisia, 1994; García del Cura  
73 et al., 2001; Hood and Wallace, 2012; Huang et al., 2014). In contrast, the absence of such signatures  
74 with a rather homogenous micritic matrix can indicate a secondary dolomite formation during early  
75 or burial diagenesis following dissolution of a primary carbonate phase or its conversion into well-  
76 ordered dolomite at a later stage. Complementary to microscopic methods, geochemical tools such  
77 as stable isotopes of oxygen, carbon or strontium were used to gain further insights in the

78 environment or the “parental fluid” in which the mineral precipitated (e.g. Land, 1980; Wilson et al.,  
79 1990; Preto et al., 2015).

80 During the last decade carbonate clumped isotope thermometry evolved as a promising tool to  
81 determine formation temperatures of carbonates and the oxygen isotope composition of the fluid  
82 source (e.g. Ghosh et al., 2006; Eiler, 2007; Ferry et al., 2011; Dale et al., 2014; Millán et al., 2016;  
83 Winkelstern and Lohmann, 2016; Rodríguez-Sanz et al., 2017; Suarez et al., 2017; Smeraglia et al.,  
84 2018). Thus it is now possible to gain important insights on the environment of carbonate mineral  
85 formation. Clumped isotope thermometry is a measure of the abundance of the  $^{13}\text{C}-^{18}\text{O}$  bond within  
86 the carbonate mineral relative to its stochastic isotope distributions, which is solely temperature  
87 dependent. Carbonate clumped isotopes are measured on the  $\text{CO}_2$  gas evolved from the reaction of  
88 the carbonate mineral with phosphoric acid as the mass 47 ( $^{13}\text{C}^{18}\text{O}^{16}\text{O}$ ). The clumped isotope  
89 composition of carbonates is thus reported in the  $\Delta_{47}$  notation:

$$\Delta_{47} = ((R^{47}/R^{47*}-1)-(R^{46}/R^{46*}-1)-(R^{45}/R^{45*}-1))*1000 (\text{‰}),$$

91 where the measured ratios between the  $m/z$  45 to 47 over the most abundant  $\text{CO}_2$  isotopologue  $m/z$   
92 44 ( $R^i$ ) are reported against their stochastic isotope distribution ( $R^{i*}$ ), which is calculated from the  
93 bulk isotope composition of the sample gas ( $\delta^{13}\text{C}$  and  $\delta^{18}\text{O}$ ). The phosphoric acid reaction of the  
94 carbonate to  $\text{CO}_2$  produces a temperature-dependent isotopic fractionation whose temperature  
95 dependence is relatively well constraint for calcite (e.g. Defliese et al., 2015; Murray et al., 2016) but  
96 not for dolomite. The temperature dependence of this acid fractionation factor (AFF) is of high  
97 importance as it is common practice to project the  $\Delta_{47}$  value to an acid digestion temperature of 25  
98 °C, the digestion temperature reported in the first clumped isotope studies (Ghosh et al., 2006) and  
99 to enable a direct comparison between different laboratories that use different acid digestion  
100 temperatures.

101 For dolomite the temperature dependence of the AFF is still debated. While earlier studies processed  
102 their  $\Delta_{47}$  measurements of different carbonate minerals with the same acid fractionation correction  
103 factors as calcite, two recent studies on the temperature dependence of the AFF for dolomite came  
104 to contrasting conclusions (Defliese et al., 2015; Murray et al., 2016). Whereas Defliese et al. (2015)  
105 observed similar temperature sensitivities for the AFF of dolomite and calcite, Murray et al. (2016)  
106 observed a much steeper temperature sensitivity for the AFF of dolomite relative to calcite. In a  
107 study on the absolute  $\Delta_{47}$  AFF at 70 °C acid digestion Müller et al. (2017a), in addition, observed  
108 significantly smaller AFF for aragonite (0.172 ‰), compared to calcite (0.197 ‰) and dolomite (0.226  
109 ‰). In this study, Müller et al. (2017a) also determined the absolute AFF for dolomite at 100 °C and  
110 observed that the dolomite acid fractionation at this temperature is smaller than the one of calcite  
111 supporting the findings of Murray et al. (2016). Interestingly, the results of Müller et al. (2017a)

112 indicate that the  $\Delta_{47}$  acid fractionation of dolomite and calcite seems to be identical at about 90 °C  
113 acid digestion temperature, the reaction temperature currently used by most clumped isotope  
114 laboratories using common acid bath systems for large samples. These inconclusive findings on the  
115  $\Delta_{47}$  acid fractionation of dolomite at different reaction temperatures can cause large uncertainties on  
116 the interpretation of the  $\Delta_{47}$  based formation temperature of dolomites, especially when comparing  
117 studies that use different acid digestion temperatures.

118 Recently two dolomite-specific  $\Delta_{47}$ -T calibrations were published (Winkelstern et al., 2016; Bonifacie  
119 et al., 2017) with the aim of eliminating additional uncertainties in the interpretation of dolomite  
120 clumped isotope temperatures. The study of Winkelstern et al. (2016) for 75 °C dolomite acid  
121 digestion revealed a slightly shallower slope than more recent and statistically more robust calcite  
122 specific calibrations (the ones corrected for negative backgrounds, in the absolute reference frame,  
123 wider calibration sample temperature range with sufficient replicates, see Fernandez et al., 2017).  
124 On the other hand, Bonifacie et al. (2017) for 90 °C acid digestion revealed that the temperature  
125 relationship of dolomite is within error of the one of calcite based on a compilation of many different  
126 published laboratories carried out in the same study. This proposed universal calibration was also  
127 statistically indistinguishable from the one for calcite of Kele et al. (2015) which was produced in our  
128 laboratory. However, the composition of the samples in Bonifacie et al. (2017) was not calculated  
129 with the new IUPAC parameters for the correction of the  $^{17}\text{O}$  abundance (Daëron et al. 2016), thus it  
130 is not clear how much the calibration would change if it were recalculated with the new parameters.  
131 A recalculation of the Kele et al. (2015) by Bernasconi et al. (2018) showed that while the slope  
132 remained constant, the intercept decreased by 0.038 ‰.

133 Due to the uncertainties in the dolomite-specific  $\Delta_{47}$  acid fractionation and its temperature-  
134 dependence and because dolomite reacts much faster at higher temperatures Bonifacie et al. (2017)  
135 published their calibration for an acid digestion temperature of 90 °C. In the ETH laboratory,  
136 dolomites and calcites are digested at 70 °C and at this temperature, a different dolomite specific  $\Delta_{47}$   
137 AFF is observed (Müller et al., 2017a). Because in many new laboratories single bath preparation  
138 systems allowing the measurement of sub-milligram samples at 70 °C are becoming the method of  
139 choice (Müller et al. 2017b, Bernasconi et al., 2018), it is crucial to produce a dolomite-specific  $\Delta_{47}$ -  
140 temperature calibration at 70 °C and to evaluate potential differences with respect to the evaluation  
141 schemes using the calcite specific parameters. In addition, in this study we firmly anchor the results  
142 to the absolute reference frame using a carbonate based correction scheme using the widely  
143 distributed ETH Standards, which allows other laboratories to better compare the data to ours  
144 (Bernasconi et al., 2018). We produced a dolomite specific  $\Delta_{47}$  temperature calibration using natural  
145 and in laboratory formed (proto-)dolomite samples covering a temperature range from 25 to 1100

146 °C. We evaluated this new calibration and show results of potential dolomite standards and the  
147 advantages of their regular analysis for an improved inter-laboratory dolomite  $\Delta_{47}$  data comparison.

148

## 149 2. MATERIALS AND METHODS

### 150 2.1. Samples

151 To cover a wide temperature range we synthesized dolomites in the laboratory under controlled  
152 temperature conditions at 70, 140 and 220 °C. For low temperature we used samples of natural  
153 dolomites formed at 25 °C from Lagoa Vermelha (Brasil) the same lagoon from which Bonifacie et al.  
154 (2017) obtained their samples. Finally, we use two dolomites that were heated in a piston cylinder to  
155 1100 °C to obtain a stochastic isotope composition. In total we analyzed 21 different samples  
156 between 6 and 87 times.

#### 157 Dolomites synthesized in the laboratory at 70, 140 and 220 °C:

158 Laboratory (proto-) dolomites were synthesized following the recipe described in Rodriguez-Blanco  
159 et al. (2015). Equimolar aqueous solutions of  $\text{Na}_2\text{CO}_3$ ,  $\text{CaCl}_2$  and  $\text{MgCl}_2$  were mixed at room  
160 temperature, which led to an instantaneous precipitation of a white, gel-like solid confirmed by X-ray  
161 diffraction to be amorphous. This gel was heated at 70, 140 and 220 °C for between 1 day and 12  
162 weeks. At selected time points, experimental runs were quenched to room temperature, the solids  
163 separated from the supernatants via vacuum-filtration (0.2  $\mu\text{m}$  polycarbonate Cyclopore filters) and  
164 dried with isopropanol. The end products were determined to be (proto-)dolomite by X-ray  
165 diffraction. Ordered crystalline dolomite forms from an initial amorphous calcium-magnesium  
166 carbonate phase that first crystallizes to a non-stoichiometric proto-dolomite, and that then  
167 transforms over hours to weeks, depending on the temperature, to fully ordered stoichiometric  
168 dolomite (Rodriguez-Blanco et al., 2015). For our calibration we analyzed multiple samples at each of  
169 the three temperatures (8 at 70 °C, 4 at 140 °C and 5 at 220 °C, respectively; see Table 1).

#### 170 Microbial dolomite concretions from the Brazilian lagoon “Lagoa Vermelha”:

171 For the low temperature range we included two dolomite concretions from a sediment core of Lagoa  
172 Vermelha (LV 15cm, LV 71cm). The lagoon is located about 100 km East of Rio de Janeiro, Brazil (Van  
173 Lith et al., 2002) and is a very shallow isolated lagoon influenced by recharge from the sea and mixing  
174 with meteoric water and evaporation which seasonally exceeds precipitation. This causes an annual  
175 wet-dry seasonal cycle with hypersaline conditions during the summer months. The dolomite  
176 concretions form during intense evaporative conditions, where the precipitation process is mediated  
177 by the increase of microbial activity and the presence of extracellular polymeric substances (EPS;

178 Nascimento, 2018). The annual mean water temperature of Lagoa Vermelha is approximately 25 °C,  
179 and the recorded temperature in 20 cm sediment depth was 25.5±5.7 °C from November 2011 till  
180 May 2015 (Nascimento, 2018) using an identical water temperature logger setup as Bahniuk et al.  
181 (2015) applied for the nearby lagoon Brejo do Espinho. These microbial dolomite samples were  
182 cleaned as in previous studies with hydrogen peroxide (10 %) and rinsed several times with deionized  
183 water to remove organic matter. This to treat them identical to a recent calibration study of  
184 (Bonifacie et al., 2017), which also included samples from Lagoa Vermelha.

185

### 186 Dolomites heated to 1100 °C in a piston cylinder:

187 Fine powder of two natural dolomites (from Monte San Salvatore, Switzerland and La Roda, Spain)  
188 were heated during 4 hours at 1100 °C in a piston cylinder apparatus. More detail on these dolomite  
189 samples with stochastic isotope distribution are in (Müller et al., 2017a) where these samples,  
190 labelled as Sansa (H) and Rodolo (H), were used to determine the absolute  $\Delta_{47}$  AFF. In this study  
191 these are the hottest calibration samples. These samples are important for a more accurate  
192 interpretation of natural dolomites that retained extremely hot temperature signals near magmatic  
193 intrusions (e.g. Lloyd et al., 2017; Ryb et al., 2017; Lloyd et al., 2018).

194

### 195 **2.2. Natural dolomites from Monte San Salvatore, Switzerland, La Roda, Spain and the** 196 **international standard NIST SRM 88b**

197 The dolomite from Monte San Salvatore, Southern Switzerland, is a replacement dolomite that  
198 formed during the middle Triassic (Lehner 1952; Zorn, 1971) and was collected along the road  
199 leading southwards from Lugano at the locality Forca di San Martino. We named the sample “Sansa”  
200 to avoid confusion with the dolomites from San Salvador Island discussed by Murray and Swart  
201 (2017).

202 The other natural sample comes from La Roda, Spain and is a lacustrine dolomite that formed during  
203 the Pliocene probably induced by microbial activity (García del Cura et al., 2001). Additionally we  
204 analyzed the NIST (National Institute of Standards and Technology, Gaithersburg, MD, USA) dolomite  
205 standard SRM 88b, which is a natural dolomite from the Silurian Racine formation, northeastern  
206 Illinois. This widely available dolomite standard was already measured in other clumped isotope  
207 studies and enables a direct comparison between different laboratories.

208

### 209 **2.3. X-ray diffraction and stable isotope analyses**

210  
211  
212  
213  
214  
215  
216  
217  
218  
219  
220  
221  
222  
223  
224  
225  
226  
227  
228  
229  
230  
231  
232  
233  
234  
235  
236  
237  
238  
239  
240  
241  
242  
243  
244  
245  
246  
247  
248  
249  
250  
251  
252  
253  
254  
255  
256  
257  
258  
259  
260  
261  
262  
263  
264  
265



210 All samples were drilled from the hand specimens with a hand-held dental drill taking care of not  
1 211 overheating the drill bit to avoid potential isotopic reordering. The mineralogy and degree of  
2 212 ordering was determined with a Powder X-ray Diffractometer Bruker AXS D8 Advance equipped with  
3 213 a Lynxeye detector. Oxygen, carbon and clumped isotope compositions were determined with a Kiel  
4 214 IV carbonate device coupled to a MAT 253 isotope ratio mass spectrometer (Thermo Fisher Scientific)  
5 215 as thoroughly described in earlier studies (Schmid and Bernasconi, 2010; Meckler et al., 2014; Müller  
6 216 et al., 2017b). Briefly, 130 to 160  $\mu\text{g}$  of calcite standards (ETH-1 to -4) and samples are weighed in  
7 217 glass vials and placed in the Kiel IV carbonate device (46 samples per measurement sequence). The  
8 218 samples are reacted at 70 °C with three drops of 104 % phosphoric acid and during the reaction with  
9 219 the acid (300 seconds for calcite and 1200 seconds for dolomite) the released  $\text{CO}_2$  gas is constantly  
10 220 frozen in the liquid nitrogen ( $\text{LN}_2$ ) trap 1 of the Kiel device. After the reaction is completed trap 1 is  
11 221 heated to -100 °C and the gas is transferred through a tubing filled with 10 mm Porapak Type Q (50-  
12 222 80 mesh) embedded in silver wool into a second  $\text{LN}_2$  trap. The Porapak trap was kept between -20  
13 223 and -14 °C to remove potential contaminants such as halo-/hydrocarbons or reduced sulfur  
14 224 compounds. The samples were measured in the LIDI mode that measures the sample gas at once for  
15 225 600 seconds and subsequently the working gas during 600 seconds. Usually the measurements start  
16 226 at 20 to 25 V on mass 44 and decrease by approx. 10 V during the 600 seconds (Hu et al., 2014;  
17 227 Müller et al., 2017b). Before starting a measurement sequence peak shape scans in the range of 30  
18 228 to 10 V on  $m/z$  44 are carried out at different gas pressures to determine the pressure dependence  
19 229 of the negative backgrounds to do a so-called pressure-sensitive baseline correction (PBL correction)  
20 230 according to (Bernasconi et al., 2013; Meckler et al., 2014; Müller et al., 2017a). The raw data are  
21 231 processed with the free Easotope software (John and Bowen, 2016), by first doing the PBL correction,  
22 232 then it calculates the carbon and oxygen isotope composition of the carbonates in the delta notation  
23 233 relative to the international Vienna PeeDee Belemnite standard, VPDB ( $\delta^{13}\text{C}_{\text{VPDB}}$ ,  $\delta^{18}\text{O}_{\text{VPDB}}$  in ‰) using  
24 234 the parameters recommended by Daëron et al., 2016). The calculated PBL-corrected clumped  
25 235 isotope composition ( $\Delta_{47\text{raw}}$ ) against our working gas ( $\delta^{13}\text{C}_{\text{VPDB}} = -7.25$  ‰,  $\delta^{18}\text{O}_{\text{VPDB}} = +1.65$  ‰) for each  
26 236 replicate was converted to  $\Delta_{47 \text{ CDES } 70 \text{ °C}}$  (‰) using 32 standards before and after. The results a  
27 237 presented as the averages of replicates measured over a long period of time, from 2015 to 2017,  
28 238 where the conditions of the analytical instruments changed several times. Our measurement  
29 239 strategy involves the measurement of only few replicates of the same sample in the same  
30 240 measurement sequence of 46 samples. The distribution of replicates over multiple runs during  
31 241 different correction intervals often comes with the cost of a worse precision compared to measuring  
32 242 many replicates of the same sample in one analytical sequence or a short time interval, but we  
33 243 expect that this leads to more accurate  $\Delta_{47}$  estimates as it removes possibly day to day biases. For  
34 244 the conversion into the absolute reference frame Easotope uses the accepted  $\Delta_{47}$  values of the  
35  
36  
37  
38  
39  
40  
41  
42  
43  
44  
45  
46  
47  
48  
49  
50  
51  
52  
53  
54  
55  
56  
57  
58  
59  
60  
61  
62  
63  
64  
65

245 calcite standards ETH-1 to -4 as reported in Bernasconi et al. (2018). Here we report the results for a  
1 246 reaction temperature of 70 °C ( $\Delta_{47}^{\text{CDES } 70 \text{ } ^\circ\text{C}}$ ) and refrain to project them to an acid digestion  
2 247 temperature of 25 °C due to the large uncertainties in the AFF of dolomite (see different  
3 248 observations in Defliese et al., 2015; Murray et al., 2016; Müller et al., 2017a). For  $\delta^{18}\text{O}$  we used a  
4 249 AFF of 1.009926 for dolomite (Rosenbaum and Sheppard, 1986). Conversion from VPDB to the  
5 250 VSMOW scale was done using  $\delta^{18}\text{O}_{\text{SMOW}} = 1.03091 * \delta^{18}\text{O}_{\text{PDB}} + 30.91$  (Coplen et al., 1983). The  $\Delta_{47}$   
6 251 temperatures of calcite samples are calculated with the fully recalculated calcite  $\Delta_{47}$ -T calibration of  
7 252 Kele et al. (2015) using the isotopic parameters recommended in Daëron et al. (2016) including the  
8 253 fully recalculated accepted ETH standard values (Bernasconi et al., 2018; with ETH-1:  $\Delta_{47} = 0.258$  ‰,  
9 254 ETH-2:  $\Delta_{47} = 0.256$  ‰, ETH-3:  $\Delta_{47} = 0.691$  ‰ and ETH-4:  $\Delta_{47} = 0.507$  ‰ projected to a 25 °C acid  
10 255 digestion using a correction factor of 0.062 ‰).

11 256 Oxygen isotopes in waters from the experiments were measured with the CO<sub>2</sub> equilibration method.  
12 257 200 µl of water are pipetted in 12 ml septum-capped vials which are subsequently filled with a  
13 258 mixture of 0.3 % CO<sub>2</sub> and He. After equilibration at 25 °C for at least 18 h the CO<sub>2</sub>/He mixture is  
14 259 measured using a Thermo Scientific Gas Bench II connected to a Thermo Scientific Delta V plus  
15 260 isotope ratio mass spectrometer. The system is calibrated with the international standards SMOW,  
16 261 SLAP and GISP. The results are reported in the conventional delta notation with respect to VSMOW  
17 262 (Coplen, 1996). Reproducibility of the measurements based on repeated measurements of an  
18 263 internal standard was better than 0.06 ‰.

19 264

### 20 265 **3. RESULTS**

#### 21 266 **3.1. Dolomite mineralogy**

22 267 The natural dolomites from Lagoa Vermelha, Brazil all show the main dolomite reflections 104, 110  
23 268 and 113 at the corresponding 2θ space and the dolomite ordering reflections 015 and 021 (Bradley et  
24 269 al., 1953; Goldsmith and Graf, 1958; Gregg et al., 2015). Whereas the ordering reflection 001 is  
25 270 lacking in the XRD pattern of LV 15 cm. In LV 71 cm there could be a small reflection but it is masked  
26 271 by a large reflection from an unidentified phase (Fig. 1). In both samples the ordering reflection 015  
27 272 is clearly smaller than the 110 reflection. In sample LV 71 cm the presence of halite (NaCl) is visible  
28 273 indicated by the green reflections at 32 and around 45 °, whereas for sample LV 15 cm it is not as  
29 274 clear as the reflection around 45 ° is not visible. With almost all dolomite ordering reflections  
30 275 expressed, the carbonate phase of LV 15 cm and LV 71 cm can be described as poorly ordered  
31 276 dolomite.

32  
33  
34  
35  
36  
37  
38  
39  
40  
41  
42  
43  
44  
45  
46  
47  
48  
49  
50  
51  
52  
53  
54  
55  
56  
57  
58  
59  
60  
61  
62  
63  
64  
65

277 The XRD patterns of the ‘dolomite samples’ synthesized in the laboratory (Table 1 and Fig. 2) at 70 °C  
278 did not show the ‘ordered’ 001, 015 and 021 dolomite reflections, pointing to a crystal structure  
279 typical for proto-dolomite which is called by some authors very high Mg-calcite (VHMC). This  
280 observation was independent of the length of equilibration at the experiment temperature of 70 °C  
281 (1 to 12 weeks). Samples crystallized at 140 °C exhibited in their XRD pattern the ‘ordered’ dolomite  
282 reflections 015 and 021, but still lacked the 001 reflection pointing to a not fully ordered dolomite.  
283 Finally, the XRD patterns of the samples synthesized at 220 °C contained all three ‘ordered’ dolomite  
284 reflections, however, the intensity of the 015 peak was relatively smaller than the 110 peak, typical  
285 for a moderately well-ordered dolomite (see lower XRD pattern in Fig. 2).

286 The dolomites NIST SRM 88b, Sansa and Rodolo are well-ordered and stoichiometric. All ordered  
287 dolomite reflections are visible and the 015 reflections are almost as intense as the 110 (Fig. 3)  
288 similar to the “near perfect ordering” example Bonneterre dolomite described in Gregg et al. (2015).  
289 The Rodolo dolomite is a direct precipitate from solution in a lacustrine environment (García del Cura  
290 et al., 2001), in contrast to the other diagenetic dolomites that are a replacement of calcite or  
291 aragonite.

### 3.2. Dolomite-water oxygen isotope fractionation

294 The averages of the measurements of all samples used for the dolomite  $\Delta_{47}$ -T calibration are  
295 displayed in Table 1 and 2 and the results of individual measurements are reported in Table S1. For  
296 the natural samples the fractionation ranges tightly between 32.01 to 32.19 ‰. The oxygen isotope  
297 composition of the water of Lagoa Vermelha is not exactly known and the value taken from van Lith  
298 et al. (2002) of 1.8 ‰ has an assigned larger uncertainty because of the annual variations in  
299 hydrology of the lagoon.

300 For the synthetic dolomites that were equilibrated with the solutions for variable times ranging from  
301 1 to 12 weeks, we obtained a larger spread in the results (70 °C samples: 21.86 - 23.23 ‰; 140 °C  
302 samples: 14.94 – 16.49 ‰; 220 °C samples: 9.66 – 13.05 ‰), thereby the water value of sample 82  
303 seems to be biased by evaporation during water sample transport prior to isotope analysis and the  
304 short 220 °C experiment Leeds 34 probably did not reach equilibrium. The uncertainty of the oxygen  
305 isotope composition of the (proto-)dolomite samples varies between  $\pm 0.03 - 0.44$  ‰ at the 95% CI,  
306 which takes into account the number of replicates per sample (indicated in last column of Table 2).

307 Table 2 shows the average  $\delta^{13}\text{C}_{\text{VPDB}}$  and  $\delta^{18}\text{O}_{\text{VPDB}}$ , the bulk isotope composition relative to our  
308 reference gas ( $\delta^{47}$ ) and the clumped isotope composition for an acid digestion temperature of 70 °C  
309 ( $\Delta_{47}^{\text{CDES } 70\text{ }^\circ\text{C}}$ ) of all samples. All uncertainties are reported at the 95% CI and range between 0.02 –

310 0.14 ‰ for  $\delta^{13}\text{C}_{\text{VPDB}}$ , 0.04 – 0.54 ‰ for  $\delta^{18}\text{O}_{\text{VPDB}}$ , 0.05 – 0.77 ‰ for  $\delta^{47}$  and 0.010 – 0.054 ‰ for  $\Delta_{47}$

311 CDES 70 °C.

312 The average  $\Delta_{47 \text{ CDES } 70 \text{ °C}}$  values of the two “cold” natural dolomite calibration samples are 0.637 ‰

313 for LV 15 cm and 0.619 ‰ for LV 71 cm, both samples have similar oxygen isotope composition, but

314 their carbon isotope compositions are more distinct with -8.32 ‰ for the more shallow sample and

315 -10.21 ‰ for the deeper one. The  $\delta^{13}\text{C}_{\text{VPDB}}$  and  $\delta^{18}\text{O}_{\text{VPDB}}$  of the synthetic samples are quite similar to

316 each other and the  $\Delta_{47 \text{ CDES } 70 \text{ °C}}$  values range between 0.497 to 0.515 ‰ for samples synthesized at 70

317 °C, between 0.398 to 0.426 ‰ for samples synthesized at 140 °C and between 0.311 to 0.348 ‰ for

318 the 220 °C samples. The two natural dolomites that were heated to 1100 °C to produce a stochastic

319 isotope distribution were replicated much more and show almost identical  $\Delta_{47 \text{ CDES } 70 \text{ °C}}$  values with

320  $0.230 \pm 0.010$  ‰ for Rodolo (H) and  $0.228 \pm 0.011$  ‰ for Sansa (H).

321 Using only the (proto-)dolomites synthesized under controlled laboratory conditions without the two

322 heated dolomites and the two natural dolomites from the Brazilian lagoon, we obtain a temperature

323 dependence with  $R^2 = 0.9862$  for the oxygen isotope fractionation relative to water of

$$10^3 \alpha_{\text{Dolomite-Water}} = 2.7757 \pm 0.2062 \times \left( \frac{10^6}{T^2} \right) - 0.6314 \pm 1.3916$$

324 For this temperature dependence we did not use sample Leeds 82 and sample Leeds 34 due to the

325 aforementioned points. The natural samples of Lagoa Vermelha were not included due to the higher

326 uncertainty in the  $\delta^{18}\text{O}$  of the fluid source.

327

### 328 3.3 Clumped isotope fractionation

329

330 The clumped isotope composition of individual replicates and averages of samples formed between

331 25 to 220 °C is plotted in Fig. 4 against their reciprocal formation temperatures ( $10^6/T^2$ ). From all

332 analyzed individual replicates we obtained a linear regression for the  $\Delta_{47 \text{ CDES } 70 \text{ °C}} - T$  relationship with

333  $R^2 = 0.8513$  of

$$\Delta_{47 \text{ CDES } 70 \text{ °C}} = 0.0426 \pm 0.0022 \times \left( \frac{10^6}{T^2} \right) + 0.1492 \pm 0.0169$$

334

335 that is valid for acid digestion of dolomites at 70 °C and the temperature in Kelvin. The linear

336 regression is based on 270 individual measurements of 19 different samples formed at 4 different

337 temperatures. Including the two measurements of the two dolomites that were heated and  
 338 equilibrated during 4 hours at 1100 °C (Müller et al., 2017a) the best fit is obtained when using a  
 339 polynomial function of third order with  $R^2 = 0.9164$

$$\Delta_{47 \text{ CDES } 70^\circ\text{C}}(\text{‰}) = -0.0002 \times \left(\frac{10^6}{T^2}\right)^3 + 0.0042 \times \left(\frac{10^6}{T^2}\right)^2 + 0.0113 \times \left(\frac{10^6}{T^2}\right) + 0.2219$$

340 based on a total of 416 individual measurements (Fig. 5).

### 342 3.4. Stable isotope data of proposed dolomite standards

343 The isotopic compositions of the three ordered dolomites are summarized in Table 3 and with the  
 344 individual replicates in the supplementary Table S2. The lacustrine Rodolo dolomite has a  $\delta^{43}\text{C}_{\text{VPDB}}$  of  
 345  $-3.71 \text{ ‰}$  and a relatively high  $\delta^{18}\text{O}_{\text{VPDB}}$  of  $2.77 \text{ ‰}$ . Because of the large number of replicates (151) the  
 346  $\Delta_{47}$  of  $0.632 \text{ ‰}$  is well constrained with an uncertainty of only  $\pm 0.006 \text{ ‰}$  at the 95% CI giving a  
 347 temperature of  $25 \pm 2 \text{ °C}$  and a fluid source with  $\delta^{18}\text{O}$  of  $+1.7 \pm 0.04 \text{ ‰}$ . The other two diagenetic  
 348 dolomites have almost identical  $\Delta_{47}$  with  $0.526 \pm 0.014 \text{ ‰}$  for Sansa and  $0.522 \pm 0.022 \text{ ‰}$  for NIST SRM  
 349 88b. Whereas their  $\delta^{13}\text{C}$  are similar, their oxygen isotope composition is different with  $-3.56 \text{ ‰}$  for  
 350 Sansa and  $-7.09 \text{ ‰}$  for NIST SRM 88b.

## 352 4. DISCUSSION

### 353 4.1. Dolomite specific $\Delta_{47}$ -temperature calibration

#### 354 4.1.1. Clumped isotope temperature relationship for 70 °C acid digestion

355 The clumped isotope analysis of 19 (proto-)dolomite samples formed at temperatures between 25  
 356 and 220 °C with phosphoric acid digestion at 70 °C resulted in a linear regression of:

$$\Delta_{47 \text{ CDES } 70^\circ\text{C}} = 0.0426 \pm 0.0022 \times \left(\frac{10^6}{T^2}\right) + 0.1492 \pm 0.0169$$

357 We start by comparing this calibration with the calcite calibration produced at ETH with the same  
 358 instrumentation and normalized to the CDES using the same carbonate standards, because we can  
 359 exclude artefacts due to methodological and data processing differences. Comparison with the  
 360 calcite calibration of Kele et al. (2015) as recalculated in Bernasconi et al. (2018), shows a slightly  
 361 shallower slope within the uncertainties of each other ( $0.0426 \pm 0.0022$  vs.  $0.0449 \pm 0.001$ ), but the  
 362 intercept of the calcite calibration is significantly lower so that the two calibrations do not overlap at  
 363 their 95% CI's (see Fig. 6). Using this calcite calibration for dolomites (between 0 and 100 °C) leads to

364 calculated temperatures lower by 10 to 16 °C compared to the dolomite-specific calibration. Thus we  
1 365 conclude that calcite and dolomite have to be treated separately when measured for clumped  
2 isotopes, and published estimates of temperatures may have to be revised. This revision would  
3 366 however also take into consideration that the original data in many publications before 2017 were  
4 367 not processed using the parameters suggested by Daëron et al. (2016), thus the effect on the  
5 368 temperatures is difficult to predict. In the following we compare our new dolomite calibration with  
6 369 Bonifacie et al. 2017.  
7 370

11 371 In the past clumped isotope analyses on natural dolomite samples were processed in the same way  
12 372 as calcite samples due to the facts that no dolomite specific  $\Delta_{47}$  temperature calibrations and no  
13 373 dolomite specific AFF were available. This was based on the assumption that the clumped isotope  
14 374 fractionation during acid digestion is identical for the two minerals (e.g. Millán et al., 2016;  
15 375 Winkelstern and Lohmann, 2016). Ferry et al. (2011) on the other hand, added a correction factor of  
16 376 0.02 ‰ and applied the theoretical calibration of Guo et al. (2009) to calculate formation  
17 377 temperatures. In recent years, two dolomite specific  $\Delta_{47}$ -T calibrations were published, one of them  
18 378 reacting dolomite at 75 °C (Winkelstern et al., 2016) and the other at 90 °C (Bonifacie et al., 2017).

21 379 The comparison of calibrations established in different laboratories remains challenging, because of  
22 380 many factors: the lack of carbonate standards to compare across laboratories, the fact that clumped  
23 381 isotope data pre-2016 are not calculated using the "Brand parameters", and the uncertainties in  
24 382 phosphoric acid fractionation (Bernasconi et al., 2018). The absolute  $\Delta_{47}$  AFF of various carbonate  
25 383 minerals was determined by Müller et al. (2017a) using carbonates with a stochastic isotope  
26 384 distribution. This study showed a that the AFF of dolomite is 29 ppm larger than the one of calcite  
27 385 and that due to the steeper temperature relationship for dolomite this difference would become  
28 386 increasingly larger at acid reaction temperatures below 90 °C. Defliese et al. (2015), on the other  
29 387 hand, determined that temperature dependence of the AFF of dolomite between 25 and 90 °C is  
30 388 identical to the one of calcite whereas Murray et al. (2016) observed a temperature dependence  
31 389 significantly steeper for dolomite.

32 390 Our new calibration allows now to address these uncertainties on potential differences of the  $\Delta_{47}$   
33 391 acid fractionation between dolomite. Because of the uncertainties in comparing data across labs  
34 392 discussed above we refrain to compare it with the Winkelstern et al. (2016) calibration, as we cannot  
35 393 directly compare any carbonate that was measured in their laboratory and we cannot recalculate it  
36 394 with the updated parameters. On the other hand we can compare our results with Bonifacie et al.,  
37 395 2017), even if that calibration is not recalculated with the new parameters because in both  
38 396 calibrations we use two samples from Lagoa Vermelha as a low temperature point, and thus we can  
39 397 directly compare the results of the two laboratories.  
40  
41  
42  
43  
44  
45  
46  
47  
48  
49  
50  
51  
52  
53  
54  
55  
56  
57  
58  
59  
60  
61  
62  
63  
64  
65

398 The calcite specific  $\Delta_{47}$ -T calibration produced at the ETH clearly lies below our new dolomite  
1 399 calibration (around 30 ppm), but their slopes are similar. The difference between the intercepts of  
2  
3 400 the dolomite and calcite calibrations produced at the ETH laboratory can be explained by the  
4  
5 401 observed differences in the absolute  $\Delta_{47}$  AFF between calcite and dolomite (Müller et al., 2017a).  
6  
7 402 However, when reevaluating the data from Müller et al. (2017a) with the new accepted ETH standard  
8  
9 403 values for consistency the offset increases to 0.04 ‰ (see Table 4, Table S3). The almost identical  
10  
11 404 slopes supports the finding that the temperature dependence of clumped isotopes is the same for all  
12  
13 405 minerals (Bonifacie et al., 2017). However, the offset of about 30 ppm shows the necessity to treat  
14  
15 406 dolomites digested at 70 °C differently than calcites. In other words dolomite formed at 25 °C would  
16  
17 407 be “made” 6 °C colder if calculated as a calcite and a dolomite formed at 80 °C would give 12 °C  
18  
19 408 colder temperatures, with also a corresponding impact on the calculated  $\delta^{48}\text{O}$  of the fluid source. A  
20  
21 409 similar offset between the  $\Delta_{47}$ -T relationship of dolomite and calcite was also predicted by  
22  
23 410 theoretical calculations of Guo et al. (2009), however, the offset was of opposite sign.

24 411 The dolomite specific  $\Delta_{47}$ -temperature calibration of Bonifacie et al. (2017) is based on 12 different  
25  
26 412 samples formed at temperatures between 25 and 350 °C with a total of 67 individual measurements  
27  
28 413 and contains one sample from Lagoa Vermelha and another one of a neighbouring lagoon (Brejo do  
29  
30 414 Espinho) that formed under similar conditions as the ones we used in this study. In their study  
31  
32 415 Bonifacie et al. (2017) reacted 5 mg samples with 104 % phosphoric acid in a common acid bath at 90  
33  
34 416 °C and obtained a linear regression of  $\Delta_{47} \text{ CDES } 90 \text{ } ^\circ\text{C} = (0.0428 \pm 0.0033) * 10^6 / T^2 + (0.1174 \pm 0.0248)$ . This  
35  
36 417 slope is almost identical to the slope of 0.0426 in this study and thus allows to directly evaluate the  
37  
38 418 clumped isotope acid fractionation correction required to compare  $\Delta_{47}$  measurements of the  
39  
40 419 different laboratories to each other. For a direct comparison between the two studies we can  
41  
42 420 compare the natural samples of Lagoa Vermelha where we obtained a  $\Delta_{47} \text{ CDES } 70 \text{ } ^\circ\text{C}$  of  $0.637 \pm 0.022$  ‰  
43  
44 421 for the upper one (LV 15cm, 16 replicates) and Bonifacie et al. (2017) obtained a  $\Delta_{47} \text{ CDES } 90 \text{ } ^\circ\text{C}$  of  
45  
46 422  $0.591 \pm 0.022$  ‰ (4 replicates) for their surface sample, an offset equal to 0.046 ‰. The average offset  
47  
48 423 between our two sediment samples from Lagoa Vermelha and their two Brazilian lagoonal samples  
49  
50 424 (CVLV and CVBE of their Table 2) would be approximately 0.029 ‰. In Fig. 7 we plotted the  
51  
52 425 temperature calibration of Bonifacie et al. (2017) with the  $\Delta_{47} \text{ CDES } 90 \text{ } ^\circ\text{C}$  against the inverse  
53  
54 426 temperature and applied the two differing published dolomite specific acid fractionations (Defliese et  
55  
56 427 al., 2015; Murray et al., 2016) to project our dolomite data to 90 °C acid digestion temperature.

57 428 Applying an acid fractionation correction (AC) of 0.0204 ‰ derived from Defliese et al. (2015), which  
58  
59 429 observed no significant differences between dolomite and calcite, our dolomite calibration lies  
60  
61 430 parallel with an offset of about 10 ppm above the one of Bonifacie et al. (2017; see Fig. 7). Whereas  
62  
63 431 with the AC of 0.0380 ‰ from Murray et al. (2016), which observed a much steeper temperature  
64  
65

432 relationship for dolomite compared to calcite, our calibration shifts down to about 8 ppm below the  
1 433 one of Bonifacie et al. (2017). The AC effectively needed to put the calibrations on the same level is  
2  
3 434 an AC of approximately 0.030 ‰, which is located somewhere in between the two temperature  
4  
5 435 sensitivity studies for dolomite and is equal to the observed average offset between our lagoonal  
6  
7 436 proto-dolomite concretions and the ones of Bonifacie et al. (2017). An additional uncertainty in this  
8  
9 437 comparison is the fact that the Bonifacie et al. (2017) was not corrected for the new “Brand “  
10  
11 438 parameters, thus the exact difference remains unclear.

12  
13 439 This example shows that applying an acid fractionation correction for  $\Delta_{47}$  analyses on dolomite can  
14  
15 440 result in large uncertainties and produce erroneous temperature estimates. Ideally laboratories apply  
16  
17 441 temperature calibrations based on dolomite samples that were acid digested at the same  
18  
19 442 temperature as already recommended by Bonifacie et al. (2017). Applying an AFF to  $\Delta_{47}$  analysis on  
20  
21 443 dolomite samples digested at 25 °C is expected to result in even larger uncertainties. The only way to  
22  
23 444 remove these uncertainties for dolomite measurements is the use of dolomite standards in addition  
24  
25 445 to calcite standards that are used to transfer the data to the CDES. The regular analysis of dolomite  
26  
27 446 standards would drastically reduce the uncertainties arising from mineral specific acid fractionation  
28  
29 447 correction and uncertainties arising from small differences in sample purification procedures and  
30  
31 448 data processing (see also Bernasconi et al., 2018). This would be valuable not only for clumped  
32  
33 449 isotopes but also for oxygen isotopes as well, as there are also uncertainties in oxygen isotope  
34  
35 450 fractionation with different preparation systems. The international NIST SRM 88b is such an example  
36  
37 451 of a dolomite that is often analyzed and two potential dolomite standards are presented below.

38  
39 452 Our dolomite specific  $\Delta_{47}$ -T calibration shows an almost identical slope than the calibration of  
40  
41 453 Bonifacie et al. (2017), which also used a mixture of high temperature stoichiometric well-ordered  
42  
43 454 dolomites and at lower temperature formed proto-dolomites. Their high temperature samples were  
44  
45 455 synthesized by placing calcite or aragonite together with Ca-Ma-(Na)-Cl solutions in stainless steel  
46  
47 456 reactor vessels that were heated for several days at the corresponding experiment temperature of  
48  
49 457 100 to 350 °C (see Horita, 2014 and Bonifacie et al., 2017). Thereby the starting carbonate phase  
50  
51 458 converts first into high-Mg calcite, then into disordered dolomite to well-ordered near stoichiometric  
52  
53 459 dolomite, which is similar to dolomite formation in this study, except that we did not use a solid  
54  
55 460 carbonate starting phase. For their low temperature calibration samples Bonifacie et al. (2017) used  
56  
57 461 similar samples than we from Brazilian hypersaline lagoons described in Vasconcelos and McKenzie,  
58  
59 462 (1997) as well as bacterially-mediated precipitated proto-dolomites that were originally used to  
60  
61 463 calibrate the oxygen isotope fractionation between the dolomite phase and the water (see  
62  
63 464 Vasconcelos et al., 2005). At intermediate temperature of 80 °C Bonifacie and colleagues precipitated  
64  
65 465 proto-dolomite from mixing solutions of  $MgSO_4$ ,  $Ca(NO_3)_2 \cdot 4H_2O$  and  $Na_2CO_3$  and keeping this mixture



466 for more than 41 days in a temperature controlled water bath. Despite the different ways forming  
467 (proto-)dolomite calibration samples the study of Bonifacie et al. and this study obtains a linear  
468 regression for the  $\Delta_{47}$ -temperature relationship that is indistinguishable. Therefore our study  
469 supports their finding that there is no difference in the  $\Delta_{47}$  between well-ordered stoichiometric  
470 dolomites and so-called proto-dolomite, or such differences if they exist, are well below the current  
471 analytical uncertainty. The minor differences to reported slopes of recent calcite specific calibrations  
472 (e.g. Bernasconi et al., 2018; Bonifacie et al., 2017; Breitenbach et al., 2018; Kelson et al., 2018; Peral  
473 et al., 2018) give further strong evidence that the slope of the clumped isotope temperature  
474 relationship is identical for different carbonates. However, for a “universal” clumped isotope  
475 calibration differences in the  $\Delta_{47}$  acid fractionation of the various carbonate mineralogies need to be  
476 taken into account, notably at lower acid digestion temperatures where these effects seem to have a  
477 bigger impact (Murray et al., 2016; Müller et al., 2017a).

478 In Fig. 8 we additionally added the two dolomite samples heated to 1100 °C to expand the dolomite  
479  $\Delta_{47}$ -T relationship at elevated temperatures that can prevail in lower crustal environment or where  
480 magmatic intrusions penetrate sedimentary rocks (e.g. Lloyd et al., 2017; Ryb et al., 2017). The  
481 resulting  $\Delta_{47}$ -T relationship is a third order polynomial fit that is largely identical to the theoretical  
482 dolomite calibration of Guo et al. (2009) displayed as grey dashed line in Fig. 8. Although the  
483 theoretical dolomite calibration of Guo et al. (2009) was calculated for 25 °C acid digestion  
484 temperature it fits well to our calibration without any correction and the small differences below 70  
485 °C and above 500 °C might be due to the fact that we do not have enough different high temperature  
486 samples between the 220 °C and the 1100 °C samples as well as at low temperatures for a better  
487 higher order polynomial fitting. The linear regression for the dolomite specific  $\Delta_{47}$ -T calibration for 70  
488 °C acid digestion fits the theoretical dolomite calibration better in the low temperature range. The  
489 striking resemblance between our polynomial fit and the theoretical calculations show the necessity  
490 of applying one or the other for dolomites exposed to temperatures above ~400 °C in natural  
491 environments. Once more the regular analysis of dolomite standards would help to correct for  
492 offsets between laboratories digesting the carbonates at different reaction temperatures allowing  
493 laboratories without own temperature calibration the application of dolomite specific  $\Delta_{47}$ -T  
494 calibrations with more confidence.

#### 495 496 **4.1.2. Oxygen isotope fractionation between (proto-)dolomites and water**

497 Dolomite is known to have a different oxygen isotope fractionation to water compared to other  
498 carbonate minerals and its temperature dependency was thoroughly studied since many decades

499 (e.g. Northrop and Clayton, 1966; Fritz and Smith, 1970; Matthews and Katz, 1977; Zheng et al.,  
1 500 1999; Vasconcelos et al., 2005; Horita, 2014). Unfortunately all of these studies faced the challenge  
2  
3 501 that in laboratory at temperatures below 100 °C it becomes difficult to synthesize dolomite, although  
4  
5 502 naturally occurring dolomite samples in most cases formed at lower temperatures (e.g. via mixing of  
6  
7 503 fluids, as diagenetic replacement phase or biologically mediated primary precipitate, see Warren et  
8  
9 504 al., 2000 for a review). Some earlier studies produced dolomite at high temperatures >100 °C and  
10  
11 505 extrapolated their results to lower temperatures (Northrop and Clayton, 1966; Matthews and Katz,  
12  
13 506 1977). Other studies precipitated with or without the help of microorganisms a carbonate phase that  
14  
15 507 is not perfect stoichiometric dolomite (Gregg et al., 2015), but this proto-dolomite phase was formed  
16  
17 508 at near surface temperatures (e.g. Fritz and Smith, 1970; Vasconcelos et al., 2005).

18 509 While these proto-dolomites are not well ordered, they show properties that distinguish them from  
19  
20 510 calcite. The cultures of Vasconcelos et al. (2005) produced a mixture of calcite and proto-dolomite  
21  
22 511 and before measurement they dissolved the calcite with EDTA, thus the Mg rich phase that has the  
23  
24 512 main 104 XRD peak in the position of a dolomite, was more resistant to dissolution than all lower Mg  
25  
26 513 calcite phases. We consider this a good indication that these phases, although not well ordered, are  
27  
28 514 not very high magnesium calcites (Kaczmarek and Thornton, 2017), but poorly ordered dolomites.

29  
30 515 Another approach to overcome the difficulty of precipitating low temperature dolomites was the  
31  
32 516 theoretical modelling of the dolomite water oxygen isotope fractionation of Zheng (1999). Other  
33  
34 517 studies, including ours, merged results from stoichiometric dolomites formed at temperatures above  
35  
36 518 140 °C with results from proto-dolomites formed at temperatures down to 70 °C (experiments down  
37  
38 519 to 80 °C in Horita, 2014). A recent study of Murray and Swart (2017) discussed and evaluated the  
39  
40 520 existing oxygen isotope calibrations for dolomite on Bahamian dolomites, on which they applied  
41  
42 521 clumped isotope thermometry. In their figure 1 they show that for dolomite of a formation  
43  
44 522 temperature of 25 °C depending on which calibration is used the  $\delta^{18}\text{O}$  of the fluid source can vary by  
45  
46 523 up to 3.6 ‰. Murray and Swart evaluated the various calibrations, by calculating the  $\delta^{18}\text{O}_{\text{fluid}}$  from  
47  
48 524 the  $\Delta_{47}$  temperature estimates and the corresponding expected  $10^3 \ln \alpha_{\text{Dolomite-Water}}$  to further test if  
49  
50 525 the results are consistent with existing dolomitization models for the Bahamian dolomites. As  
51  
52 526 outcome of their study they favor the use of the temperature relationship of Matthews and Katz  
53  
54 527 (1977) for their Bahamian dolomites that presumably formed at temperatures between 15 to 35 °C.  
55  
56 528 They ignore the low temperature dolomite calibrations covering this temperature range arguing that  
57  
58 529 they were based on proto-dolomites or very-high Mg-calcite samples (Fritz and Smith, 1970;  
59  
60 530 Vasconcelos et al., 2005).

59 531 The direct comparison of these studies on the temperature dependency of the oxygen isotope  
60  
61 532 fractionation between dolomite and water is however difficult because they applied different acid  
62  
63  
64  
65

533 fractionation factors. In our study, we applied the acid fractionation factor correction for dolomite of  
1 534 Rosenbaum and Sheppard (1986), same as the two most recent studies of Vasconcelos et al. (2005)  
2  
3 535 and Horita (2014). In contrast to that Northrop and Clayton (1966) use for 25 °C acid digestion a  
4  
5 536 correction factor of 1.01090 and Fritz and Smith (1970) use at identical reaction temperature for  
6  
7 537 their proto-dolomites the calcite acid fractionation factor of 1.01008 (both derived from Sharma and  
8  
9 538 Clayton, 1965) and Matthews and Katz (1977) us for 25 °C acid digestion a factor of 1.01110 (from  
10  
11 539 Friedman and O’Neil, 1977). Further uncertainties might originate from the oxygen isotope analyses  
12  
13 540 of the water when comparing studies published during almost half a century. In Fig. 9 we compiled  
14  
15 541 the oxygen isotope fractionation between (proto-)dolomites and water of this study with the two  
16  
17 542 most recently published temperature relationships that applied the same acid fractionation  
18  
19 543 correction (Vasconcelos et al., 2005; Horita, 2014) together with the temperature relationship of  
20  
21 544 Matthews and Katz (1977) recommended in the study of Murray and Swart (2017). For this  
22  
23 545 calibration we applied a correction factor of -0.68 ‰ to the intercept of their temperature  
24  
25 546 relationship to correct for the different acid fractionations. The factor of -0.68 ‰ is the difference  
26  
27 547 between the acid fractionation factor used by Matthews and Katz (1977) and the one for 25 °C acid  
28  
29 548 digestion of Rosenbaum and Sheppard (1986). From this figure it appears that our new experimental  
30  
31 549 data overlap well with those of Vasconcelos et al. (2005) and Horita (2014), whereas the Matthews  
32  
33 550 and Katz (1977) calibration is slightly below the data compilation over the entire temperature range.  
34  
35 551 Because of the uncertainties in the  $\delta^{18}\text{O}_{\text{H}_2\text{O}}$  of water from Lagoa Vermelha we do not include the  
36  
37 552 oxygen isotope fractionations of these two natural samples in the temperature calibration in Fig. 9.

36 553 The study of Horita (2014) contains samples that cover a temperature range from 80 to 350 °C,  
37  
38 554 whereas the study of Vasconcelos et al. (2005) covers a temperature range of 25 to 45 °C with a  
39  
40 555 slightly more shallow temperature relationship. If the results of the proto-dolomites precipitated  
41  
42 556 between 25 to 79 °C of Fritz and Smith (1970) are corrected for the difference of their applied acid  
43  
44 557 fractionation at 25 °C, their calibration line is parallel to but slightly below the one of Vasconcelos et  
45  
46 558 al. (2005).

47 559 Due to the before mentioned points and the similarity of our dataset with the two most recent  
48  
49 560 studies (Vasconcelos et al., 2005 and Horita, 2014) we propose to combine the results of these three  
50  
51 561 studies to derive a more accurate temperature dependence of the water-dolomite oxygen isotope  
52  
53 562 fractionation because it is based on more data points and covers a wide temperature range of 25 to  
54  
55 563 350 °C (see Fig. 9). Based on observations from the statistical evaluation of Fernandez et al. (2017) of  
56  
57 564 existing  $\Delta_{47}$ -T calibrations that more samples covering a wider temperature range lead to more  
58  
59 565 robust calibrations we therefore recommend to use this combined  $10^3 \ln \alpha_{\text{Dolomite-Water-T}}$  relationship

60  
61 566  $10^3 \ln \alpha_{\text{Dolomite-Water}} = 2.9923 \pm 0.0557 \times (10^6/T^2) - 2.3592 \pm 0.4116$   
62  
63  
64  
65

567 to calculate the  $\delta^{18}\text{O}$  of the fluid source of unknown samples. This makes extrapolations from  
568 calibrations based on high temperature dolomite samples to lower temperatures unnecessary.

### 570 **4.3. New dolomite standards for improved inter-laboratory comparison**

571 The comparison of the new dolomite specific  $\Delta_{47}$ -T calibration of this study for 70 °C acid digestion  
572 with the calibration of Bonifacie et al. (2017) where they digested their dolomite samples at 90 °C  
573 shows that the discrepancy is due to poorly constrained understanding of the temperature  
574 dependence of the AFF for dolomite and possibly the use of the new Brand parameters, but the slope  
575 of the calibration is statistically indistinguishable. We observed a larger difference to the calibration  
576 of Winkelstern et al. (2016) (difference in slope and intercept) although it was realized with acid  
577 digestion temperature of 75 °C, closer to ours. This points to other unknown factors in the sample  
578 preparation or data processing as cause for the discrepancy, which may be overcome with carbonate  
579 standards (Bernasconi et al., 2018). These observed differences together with the inconclusive  
580 comparisons to other dolomite  $\Delta_{47}$ -fluid inclusion studies that used calcite specific  $\Delta_{47}$ -T calibrations  
581 (Came et al., 2017; Honlet et al., 2017) underline the urgent need of dolomite standards to reduce  
582 the uncertainties between laboratories. Simultaneous measurements of multiple dolomite standards  
583 with different bulk isotope composition and different  $\Delta_{47}$  allows to detect differences due to  
584 stretching or background correction or calculations to transfer the isotope results to the CDES (see  
585 Bernasconi et al., 2018 for a detailed discussion of the advantages of carbonate standards). In  
586 addition, these dolomite standards, will help solving uncertainties in oxygen isotope fractionation.  
587 We propose three possible standards that have a range of compositions for this. Besides the already  
588 available NIST SRM 88b dolomite standard ( $\Delta_{47}$  CDES 70 °C of  $0.522\pm 0.022$  ‰) that is distributed by the  
589 National Institute of Standards and Technology (Gaithersburg, MD, USA), we propose two potentially  
590 new dolomite standards, the lacustrine low temperature Rodolo dolomite ( $\Delta_{47}$  CDES 70 °C of  $0.632\pm 0.006$   
591 ‰) and the warmer Sansa dolomite ( $\Delta_{47}$  CDES 70 °C of  $0.526\pm 0.014$  ‰), which is the product of  
592 diagenetic alteration of a primary marine carbonate (Table 3). All of these three dolomites show the  
593 XRD patterns of well-ordered stoichiometric dolomite (Fig. 3). The Rodolo and Sansa can be obtained  
594 directly from Stefano Bernasconi (stefano.bernasconi@erdw.ethz.ch). Rodolo and Sansa were also  
595 analyzed for their  $\Delta_{47}$  in the laboratory of the MIT with a Nu Perspective mass spectrometer coupled  
596 to a Nu Carb device by Kristin D. Bergmann and reproduced well the results of the ETH laboratory  
597 (see Bernasconi et al., 2018).

## 599 **5. CONCLUSIONS**

600 Our dolomite specific  $\Delta_{47}$ -T calibration for 70 °C acid digestion temperature covers a wide  
1 601 temperature range from 25 to 1100 °C and is based on 21 different (proto-)dolomite samples that  
2 602 formed at known temperatures and consists of a total of 416 individual measurements. This new  
3 603 dolomite calibration has identical slope but an offset of about 30 ppm to the one of Bonifacie et al.  
4 604 (2017) for 90 °C digestion. This offset corresponds to the dolomite isotope fractionation correction  
5 605 for acid digestions at 70 °C and 90 °C and lies in between the ones reported by Defliese et al. (2015)  
6 606 with a calcite similar behavior and by Murray et al. (2016) with a dolomite reaction temperature  
7 607 sensitivity much steeper than for calcite. However, the obtained offset of 30 ppm might change if the  
8 608 dataset of Bonifacie et al. (2017) will be recalculated with the newly recommended isotopic  
9 609 parameters (“Brand” parameters).

10 610 Comparing the novel dolomite specific  $\Delta_{47}$ -T calibration to the calcite specific calibration of the same  
11 611 laboratory (Bernasconi et al., 2018) back-projected to 70 °C acid digestion, we observe a clear offset  
12 612 of about 30 ppm in average in the temperature range of 5 to 95 °C, whereas the slopes of both  
13 613 calibrations are within their uncertainties (0.0426±0.0022 for dolomite vs. 0.0449±0.001 for calcite).  
14 614 The offset between the two calibration sets corresponds to the different absolute  $\Delta_{47}$  acid  
15 615 fractionations of dolomite and calcite already observed in Müller et al. (2017a).

16 616 We also propose a new dolomite-water oxygen fractionation equation based on samples from this  
17 617 study and from Vasconcelos et al. (2005) and Horita (2014) valid for temperatures between 25 and  
18 618 350 °C.

19 619 The observed differences between the two carbonate mineralogies and the uncertainties in  
20 620 correcting  $\Delta_{47}$  and  $\delta^{18}\text{O}$  analyses of dolomites for different acid digestion temperatures underline the  
21 621 necessity of using dolomite specific  $\Delta_{47}$ -T calibrations ideally constructed at identical sample reaction  
22 622 temperatures. The regular analysis of dolomite standards would also enable the use of dolomite  
23 623 specific  $\Delta_{47}$ -T calibrations done in other laboratories and in general would allow a much better data  
24 624 comparison between different laboratories.

25 625

## 26 626 **ACKNOWLEDGMENTS**

27 627 We would like to thank Stewart Bishop and Madalina Jaggi for the support and maintenance of our  
28 628 laboratory, Magali Bonifacie for thorough discussions on the natural dolomite samples we used for  
29 629 our calibration and Lukas A. Müller for helpful hands and “bonne courage” during a Latemar field  
30 630 campaign under difficult conditions. We appreciate the detailed information of Robert D. Vocke Jr.  
31 631 on the NIST SRM 88b dolomite standard. The work was funded by the Swiss National Science  
32 632 Foundation Project No 200020\_160046 to SB. Inigo A. Müller is also very thankful for the financial

633 support by Prof. Heather Stoll, which allowed him to finish this project. Liane G. Benning  
634 acknowledges funding from the German Helmholtz Recruiting Initiative (award number I-044-16-01)  
635 and the Marie Curie EU-FP6 MIN-GRO Research and the Training Network under contract MRTN-CT-  
636 2006-035488.

637

## 638 REFERENCES

639 Assonov S. and Brenninkmeijer C. (2003) A redetermination of absolute values for  $^{17}\text{R}_{\text{VPDB-CO}_2}$  and  
640  $^{17}\text{R}_{\text{VSMOW}}$ . *Rapid Communication to Mass Spectrometry* **17**, 1017-1029.

641 Baertschi P. (1976) Absolute  $^{18}\text{O}$  content of standard mean ocean water. *Earth and Planetary Science*  
642 *Letters* **31**, 341-344.

643 Bahniuk A., McKenzie J.A., Perri E., Bontognali T.R.R., Vögeli N., Rezende C.E., Rangel T.P. and  
644 Vasconcelos C. (2015) Characterization of environmental conditions during microbial Mg-  
645 carbonate precipitation and early diagenetic dolomite crust formation: Brejo do Espinho, Rio  
646 de Janeiro, Brazil. From Bosence D.W.J., Gibbons K.A., LeHeron D.P., Morgan W.A., Pritchard  
647 T. and Vining B.A. (eds). *Microbial Carbonates in Space and Time: Implications for Global*  
648 *Exploration and Production*. Geological Society, London, Special Publications, **418**, 243-259.

649 Barkan E. and Luz B. (2005) High-precision measurements of  $^{17}\text{O}/^{16}\text{O}$  ratios in  $\text{H}_2\text{O}$ . *Rapid*  
650 *Communications to Mass Spectrometry* **26**, 2733-2738.

651 Bernasconi S.M. (1991) Geochemical and microbial controls on dolomite formation and organic  
652 matter production/preservation in anoxic environments: a case study from the Middle  
653 Triassic Grenzbitumenzone, Southern Alps (Ticino, Switzerland). Dissertation ETH No. 9432.

654 Bernasconi S.M., Hu B., Wacker U., Fiebig J., Breitenbach S.F.M. and Rutz T. (2013) Background  
655 effects on Faraday collectors in gas-source mass spectrometry and implications for clumped  
656 isotope measurements. *Rapid Communications to Mass Spectrometry* **27**, 603-612.

657 Bernasconi S.M., Müller I.A., Bergmann K.D., Breitenbach S.F.M., Fernandez A., Hodell D.A., Jaggi M.,  
658 Meckler A.N., Millan I. and Ziegler M. (2018) Reducing uncertainties in carbonate clumped  
659 isotope analysis through consistent carbonate-based standardization. *Geochemistry,*  
660 *Geophysics, Geosystems* **19**, 2895-2914.

661 Berra F., Jadoul F. and Anelli A. (2010) Environmental control on the end of the Dolomia  
662 Principale/Hauptdolomit depositional system in the central Alps: Coupling sea-level and  
663 climate changes. *Paleogeography, Palaeoclimatology, Palaeoecology* **290**, 138-150.

- 664 Bonifacie M., Calmels D., Eiler J. M., Horita J., Chaduteau C., Vasconcelos C., Agrinier P., Katz A.,  
1 665 Passey B. H., Ferry J. M. and Bourrand J.-J. (2017) Calibration of the dolomite clumped  
2 isotope thermometer from 25 to 350 °C, and implications for a universal calibration for all  
3 666 isotope thermometer from 25 to 350 °C, and implications for a universal calibration for all  
4 (Ca, Mg, Fe)CO<sub>3</sub> carbonates. *Geochimica et Cosmochimica Acta* **200**, 255-279.  
5 667  
6  
7 668 Bontognali T.R.R., Vasconcelos C., Warthmann R.J., Bernasconi S.M., Dupraz C., Strohmenger C.J. and  
8 669 McKenzie J.A. (2010) Dolomite formation within microbial mats in the coastal sabkha of Abu  
9 Dhabi (United Arab Emirates). *Sedimentology* **57**, 824-844.  
10 670  
11  
12 671 Brauchli M., McKenzie J.A., Strohmenger C.J., Sadooni F., Vasconcelos C., Bontognali T.R.R. (2016) The  
13 importance of microbial mats for dolomite formation in the Dohat Faishakh sabkha, Qatar. *Carbonates  
14 672 and Evaporites* **31** (3), 339-345.  
15 673  
16  
17 674 Bradley W.F., Burst J.F. and Graf D.L. (1953) Crystal chemistry and differential thermal effects of  
18 dolomite. *American Mineralogist* **38**, 207-217.  
19 675  
20  
21 676 Breitenbach S.F.M., Mleneck-Vautravers M.J., Grauel A.-L., Lo L., Bernasconi S.M., Müller I.A., Rolfe J.,  
22 Gázquez F., Greaves M. and Hodell D.A. (2018) Coupled Mg/Ca and clumped isotope analyses  
23 677 of foraminifera provide consistent water temperatures. *Geochimica et Cosmochimica Acta*  
24 678 **236**, 283-296.  
25 679  
26  
27 680 Bristow T. F., Bonifacie M., Derkowski A., Eiler J. M. and Grotzinger J. P. (2011) A hydrothermal origin  
28 681 for isotopically anomalous cap dolostone cements from south China. *Nature* **474**, 68-71.  
29 682  
30  
31 683 Burns S.J., McKenzie J.A. and Vasconcelos C. (2000) Dolomite formation and biogeochemical cycles in  
32 the Phanerozoic. *Sedimentology* **47**, 49-61.  
33 684  
34  
35 685 Came R.E., Azmy K., Tripathi A. and Olanipekun B.-J. (2017) Comparison of clumped isotope signatures  
36 686 of dolomite cements to fluid inclusion thermometry in the temperature range of 73-176 °C.  
37 *Geochimica et Cosmochimica Acta* **199**, 31-47.  
38 687  
39  
40 688 Chai L., Navrotsky A. and Reeder R.J. (1995) Energetics of calcium-rich dolomite. *Geochimica et  
41 689 Cosmochimica Acta* **59**, 939-944.  
42 690  
43  
44 691 Chang T. and Li W. (1990) A calibrated measurement of the atomic weight of carbon. *Chinese Science  
45 692 Bulletin* **35**, 290-296.  
46 693  
47  
48 694 Cocker J.D., Griffin B.J. and Muehlenbachs K. (1982) Oxygen and carbon isotope evidence for  
49 695 seawater-hydrothermal alteration of the Macquarie Island ophiolite. *Earth and Planetary  
50 696 Science Letters* **61**, 112-122.  
51 697  
52  
53  
54  
55  
56  
57  
58  
59  
60  
61  
62  
63  
64  
65

- 694 Coplen T.B., Kendall C. and Hopple J. (1983) Comparison of stable isotope reference samples. *Nature*  
1 695 **302**, 236-238.  
2  
3
- 4 696 Coplen T.B. (1996) Atomic weights of the elements 1995 (Technical report). *Pure and Applied*  
5 697 *Chemistry* **68**, 2339-2359.  
6  
7
- 8 698 Daëron M., Blamart D., Peral M. and Affek H.P. (2016) Absolute isotopic abundance ratios and the  
9 699 accuracy of  $\Delta_{47}$  measurements. *Chemical Geology* **442**, 83-96.  
10  
11
- 12 700 Dale A., John C.M., Mozley P.S., Smalley P.C. and Muggeridge A.H. (2014) Time-capsule concretions:  
13 701 Unlocking burial diagenetic processes in the Mancos Shale using carbonate clumped  
14 702 isotopes. *Earth and Planetary Science Letters* **394**, 30-37.  
15  
16  
17
- 18 703 Defliese W. F., Hren M. T. and Lohmann K. C. (2015) Compositional and temperature effects of  
19 704 phosphoric acid fractionation on  $\Delta_{47}$  analysis and implications for discrepant calibrations.  
20 705 *Chemical Geology* **396**, 51-60.  
21  
22  
23
- 24 706 Del Cura M. A. G., Calvo J. P., Ordóñez S., Jones B. F. and Cañaveras J. C. (2001) Petrographic and  
25 707 geochemical evidence for the formation of primary, bacterially induced lacustrine dolomite:  
26 708 La Roda 'white earth' (Pliocene, central Spain). *Sedimentology* **48**, 897-915.  
27  
28  
29
- 30 709 Dennis K. J., Affek H. P., Passey B. H., Schrag D. P. and Eiler J. M. (2011) Defining an absolute  
31 710 reference frame for "clumped" isotope studies of CO<sub>2</sub>. *Geochimica et Cosmochimica Acta* **75**,  
32 711 7117–7131.  
33  
34  
35
- 36 712 Do Nascimento G.S. (2018) Influence of climatic and oceanographic conditions on bio-mineralization  
37 713 processes in hypersaline coastal lagoons (Rio de Janeiro – Brazil), Dissertation ETH.  
38  
39  
40
- 41 714 Eiler J.M. (2007) "Clumped-isotope" geochemistry-The study of naturally-occurring, multiply-  
42 715 substituted isotopologues. *Earth and Planetary Science Letters* **262**, 309-327.  
43  
44
- 45 716 Epstein S. and Mayeda T. (1953) Variations of the O<sup>18</sup>/O<sup>16</sup> ratio in natural waters. *Geochimica et*  
46 717 *Cosmochimica Acta* **4**, 213-224.  
47  
48
- 49 718 Fernandez A., Müller I.A., Rodríguez-Sanz L., van Dijk J., Looser N. and Bernasconi S.M. (2017) A  
50 719 reassessment of the precision of carbonate clumped isotope measurements: implications for  
51 720 calibrations and paleoclimate reconstructions. *Geochemistry, Geophysics, Geosystems* **18**,  
52 721 4375-4386.  
53  
54  
55
- 56 722 Ferry J. M., Passey B. H., Vasconcelos C. and Eiler J. M. (2011) Formation of dolomite at 40-80 °C in  
57 723 the Latemar carbonate buildup, Dolomites, Italy, from clumped isotope thermometry.  
58 724 *Geology* **39**, 571-574.  
59  
60  
61  
62  
63  
64  
65



- 725 Friedman I. and O'Neil J.R. (1977) Compilation of stable isotope fractionation factors of geochemical  
1 726 interest. Eds. Fleischer M., In Data of Geochemistry. Sixth Edition. *Geological Survey*  
2 *Professional Paper 440*, KK1-KK9.  
3  
4  
5  
6 728 Frisia S. (1994) Mechanisms of complete dolomitization in a carbonate shelf: comparison between  
7  
8 729 the Norian Dolomia Principale (Italy) and the Holocene of Abu Dhabi Sabkha. *Special*  
9 *Publication International Association of Sedimentologists 21*, 55-74.  
10  
11  
12 731 Fritz P. and Smith D.G.W. (1970) The isotopic composition of secondary dolomites. *Geochimica et*  
13 *Cosmochimica Acta 34*, 1161-1173.  
14  
15  
16 733 García del Cura A.M., Calvo J.P., Ordóñez S., Jones B.F. and Cañaveras J.C. (2001) Petrographic and  
17  
18 734 geochemical evidence for the formation of primary, bacterially induced lacustrine dolomite:  
19  
20 735 La Roda 'white earth' (Pliocene, central Spain). *Sedimentology 48*, 897-915.  
21  
22 736 Ghosh P., Adkins J., Affek H., Balta B., Guo W., Schauble E.A., Schrag D. and Eiler J.M. (2006) <sup>13</sup>C-<sup>18</sup>O  
23  
24 737 bonds in carbonate minerals: A new kind of paleothermometer. *Geochimica et Cosmochimica*  
25 *Acta 70*, 1439-1456.  
26  
27  
28 739 Goldsmith J.R. and Graf D.L. (1958) Structural and compositional variations in some natural  
29  
30 740 dolomites. *The Journal of Geology 66*, 678-693.  
31  
32  
33 741 Given R.K. and Wilkinson B.H. (1987) Dolomite abundance and stratigraphic age, constraints on rates  
34  
35 742 and mechanisms of dolostone formation. *Journal of Sedimentary Petrology 57*, 1068-  
36 1078. Gregg J. M., Bish D. L., Kaczmarek S. E. and Machel H. G. (2015) Mineralogy, nucleation  
37  
38 744 and growth of dolomite in the laboratory and sedimentary environment: A review.  
39  
40 745 *Sedimentology 62*, 1749-1769.  
41  
42 746 Guo W., Mosenfelder J.L., Goddard III W.A. and Eiler J.M. (2009) Isotopic fractionations associated  
43  
44 747 with phosphoric acid digestion of carbonate minerals: Insights from first-principles  
45  
46 748 theoretical modeling and clumped isotope measurements. *Geochimica et Cosmochimica Acta*  
47 *73*, 7203-7225.  
48  
49  
50 750 Hardie L.A. (1996) Secular variation in seawater chemistry: an explanation for the coupled secular  
51  
52 751 variation in the mineralogies of marine limestones and potash evaporates over the past 600  
53  
54 752 m.y. *Geology 24*, 279-283.  
55  
56 753 Hood A.vS., Wallace M.W. and Drysdale R.N. (2011) Neoproterozoic aragonite-dolomite seas?  
57  
58 754 Widespread marine dolomite precipitation in Cryogenian reef complexes. *Geology 39*, 871-  
59  
60 755 874.  
61  
62  
63  
64  
65

- 756 Hood A.vS. and Wallace M.W. (2012) Synsedimentary diagenesis in a Cryogenian reef complex:  
1 757 Ubiquitous marine dolomite precipitation. *Sedimentary Geology* **255-256**, 56-71.  
2  
3
- 4 758 Holland H.D., Horita J. and Seyfried W. (1996) On the secular variations in the composition of  
5  
6 759 Phanerozoic marine potash evaporates. *Geology* **24**, 993-996.  
7
- 8 760 Honlet R., Gasparrini M., Muchez P., Swennen R. and John C.M. (2017) A new approach to  
9  
10 761 geobarometry by combining fluid inclusion and clumped isotope thermometry in  
11  
12 762 hydrothermal carbonates. *Terra Nova* **30**, 199-206.  
13
- 14 763 Horita J. (2014) Oxygen and carbon isotope fractionation in the system dolomite-water-CO<sub>2</sub> to  
15  
16 764 elevated temperatures. *Geochimica et Cosmochimica Acta* **129**, 111-124.  
17
- 18 765 Huang S., Huang K., Lü J. and Lan Y. (2014) The relationship between dolomite textures and their  
19  
20 766 formation temperature: a case study from the Permian-Triassic of the Sichuan Basin and the  
21  
22 767 Lower Paleozoic of the Tarim Basin. *Petroleum Science* **11**, 39-51.  
23
- 24 768 Hu B., Radke J., Schlüter H.-J., Heine F.T., Zhou L. and Bernasconi S.M. (2014) A modified procedure  
25  
26 769 for gas-source isotope ratio mass spectrometry: the long-integration dual-inlet (LIDI)  
27  
28 770 methodology and implications for clumped isotope measurements. *Rapid Communications to*  
29  
30 771 *Mass Spectrometry* **28**, 1413-1425.  
31
- 32 772 John C. M. and Bowen D. (2016) Community software for challenging isotope analysis: First  
33  
34 773 applications of “Easotope” to clumped isotopes. *Rapid Communications to Mass*  
35  
36 774 *Spectrometry* **30**, 2285–2300.  
37
- 38 775 Kaczmarek E.S. and Thornton B.P. (2017) The effect of temperature, cation ordering, and reaction  
39  
40 776 rate in high-temperature dolomitization experiments. *Chemical Geology* **468**, 32-41.  
41  
42
- 43 777 Katz A., Bonifacie M., Hermoso M., Cartigny P. and Calmels D. (2017) Laboratory-grown coccoliths  
44  
45 778 exhibit no vital effect in clumped isotope ( $\Delta 47$ ) composition on a range of geologically  
46  
47 779 relevant temperatures. *Geochimica et Cosmochimica Acta* **208**, 335–353.  
48
- 49 780 Kele S., Breitenbach S. F. M., Capezzuoli E., Meckler A. N., Ziegler M., Millan I. M., Kluge T., Deák J.,  
50  
51 781 Hanselmann K., John C. M., Yan H., Liu Z. and Bernasconi S. M. (2015) Temperature  
52  
53 782 dependence of oxygen- and clumped isotope fractionation in carbonates: A study of  
54  
55 783 travertines and tufas in the 6-95 °C temperature range. *Geochimica et Cosmochimica Acta*  
56  
57 784 **168**, 172-192.  
58  
59  
60  
61  
62  
63  
64  
65

- 785 Kelson J.R., Huntington K.W., Schauer A.J., Saenger C. and Lechler A.R. (2017) Toward a universal  
1 786 carbonate clumped isotope calibration: Diverse synthesis and preparatory methods suggest a  
2  
3 787 single temperature relationship. *Geochimica et Cosmochimica Acta* **197**, 104-131.  
4
- 5  
6 788 Kim S.-T. and O'Neil J.R. (1997) Equilibrium and nonequilibrium oxygen isotope effects in synthetic  
7  
8 789 carbonates. *Geochimica et Cosmochimica Acta* **61**, 3461-3475.  
9
- 10 790 Kluge T., John C.M., Jourdan A.-L., Davis S. and Crawshaw J. (2015) Laboratory calibration of the  
11  
12 791 calcium carbonate clumped isotope thermometer in the 25-250 °C temperature range.  
13  
14 792 *Geochimica et Cosmochimica Acta* **157**, 213-227.  
15
- 16 793 Land L.S. (1980) The isotopic and trace element geochemistry of dolomite: the state of the art. In:  
17  
18 794 Zenger D.H., Dunham J.B. and Ethington R.L. (Eds.), Concepts and Models of Dolomitization.  
19  
20 795 Spec. Publ. –*SEPM* **28**, 87-110.  
21
- 22 796 Land L.S. (1985) The origin of massive dolomite. *Journal of Geological Education* **33**, 112-125.  
23
- 24 797 Land L.S. (1998) Failure to precipitate dolomite at 25 degrees C from dilute solution despite 1000-fold  
25  
26 798 oversaturation after 32 years. *Aquatic Geochemistry* **4**, 361-368.  
27
- 28  
29 799 Lehner P. (1952) Zur Geologie des Gebietes der Denti della Vecchia, des M. Boglia, des M. Brè, und  
30  
31 800 des Monte Salvatore bei Lugano. *Eclogae geol. Helv.* **45**, 86–159.  
32
- 33 801 Lloyd M.K., Eiler J.M. and Nabelek P.I. (2017) Clumped isotope thermometry of calcite and dolomite  
34  
35 802 in a contact metamorphic environment. *Geochimica et Cosmochimica Acta* **197**, 323-344.  
36
- 37 803 Lloyd M.K., Ryb U. and Eiler J.M. (2018) Experimental calibration of clumped isotope reordering in  
38  
39 804 dolomite. *Geochimica et Cosmochimica Acta* **242**, 1-20.  
40
- 41  
42 805 Matthews A. and Katz A. (1977) Oxygen isotope fractionation during the dolomitization of calcium  
43  
44 806 carbonate. *Geochimica et Cosmochimica Acta* **41**, 1431-1438.  
45
- 46 807 Meckler A. N., Ziegler M., Millán M. I., Breitenbach S. F. M. and Bernasconi S. M. (2014) Long-term  
47  
48 808 performance of the Kiel carbonate device with a new correction scheme for clumped isotope  
49  
50 809 measurements. *Rapid Commun. Mass Spectrom.* **28**, 1705–1715.  
51
- 52 810 Millán I.M., Machel H.G. and Bernasconi S.M. (2016) Constraining temperatures of formation and  
53  
54 811 composition of dolomitizing fluids in the Upper Devonian Nisku Formation (Alberta, Canada)  
55  
56 812 with clumped isotopes. *Journal of Sedimentary Research* **86**, 107-112.  
57
- 58 813 Muehlenbachs K. and Clayton R.N. (1976) Oxygen isotope composition of the oceanic crust and its  
59  
60 814 bearing on seawater. *Journal of Geophysical Research* **81**, 4365-4369.  
61  
62  
63  
64  
65

- 815 Müller I. A., Violay M. E. S., Storck J. C., Fernandez A., van Dijk J., Madonna C. and Bernasconi S. M.  
1 816 (2017a) Clumped isotope fractionation during phosphoric acid digestion of carbonates at 70 °C.  
2  
3 817 *Chem. Geol.* **449**, 1–14.  
4  
5  
6 818 Müller I. A., Fernández A., Radke J., van Dijk J., Bowen D., Schwieters J. and Bernasconi S. (2017b)  
7  
8 819 Carbonate clumped isotope analyses with the Long-integration dual-inlet (LIDI) workflow:  
9  
10 820 Scratching at the lower sample weight boundaries. *Rapid Communications to Mass Spectrometry*  
11 821 **31**, 1057-1066.  
12  
13  
14 822 Murray S. T., Arienzo M. M. and Swart P. K. (2016) Determining the  $\Delta_{47}$  acid fractionation in  
15 823 dolomites. *Geochimica et Cosmochimica Acta* **174**, 42-53.  
16  
17  
18 824 Murray S.T. and Swart P.K. (2017) Evaluating formation fluid models and calibrations using clumped  
19 825 isotope paleothermometry on Bahamian dolomites. *Geochimica et Cosmochimica Acta* **206**,  
20 826 73-93.  
21  
22  
23  
24 827 Northrop D.A. and Clayton R.N. (1966) Oxygen-isotope fractionations in systems containing dolomite.  
25 828 *The Journal of Geology* **74**, 174-196.  
26  
27  
28 829 Peral M., Daëron M., Blamart D., Bassinot F., Dewilde F., Smialkowski N., Isguder G., Bonnin J.,  
29 830 Jorissen F., Kissel C., Michel E., Vázquez Riveiros N. and Waelbroeck C. (2018) Updated  
30 831 calibration of the clumped isotope thermometer in planktonic and benthic foraminifera.  
31 832 *Geochimica et Cosmochimica Acta* **239**, 1-16.  
32  
33  
34  
35  
36 833 Preto N., Breda A., dal Corso J., Spötl C., Zorzi F. and Frisia S. (2015) Primary dolomite in the Late  
37 834 Triassic Travenanzes Formation, Dolomites, Northern Italy: Facies control and possible  
38 835 bacterial influence. *Sedimentology* **62**, 697-716.  
39  
40  
41  
42 836 Rodríguez-Blanco J. D., Shaw S. and Benning L. G. (2015) A route for the direct crystallization of  
43 837 dolomite. *American Mineralogist* **100**, 1172-1181.  
44  
45  
46 838 Rodríguez-Sanz L., Bernasconi S.M., Marino G., Heslop D., Müller I.A., Fernandez A., Grant K.M. and  
47 839 Rohling E.J. (2017) Penultimate deglacial warming across the Mediterranean Sea revealed by  
48 840 clumped isotopes in foraminifera. *Scientific Reports* **7**: 16572, 1-11.  
49  
50  
51  
52 841 Rosenbaum J. and Sheppard S. M. (1986) An isotopic study of siderites, dolomites and ankerites at  
53 842 high temperatures. *Geochimica et Cosmochimica Acta* **50**, 1147-1150.  
54  
55  
56  
57 843 Ryb U., Lloyd M.K., Stolper D.A. and Eiler J.M. (2017) The clumped-isotope geochemistry of exhumed  
58 844 marbles from Naxos, Greece. *Earth and Planetary Science Letters* **470**, 1-12.  
59  
60  
61  
62  
63  
64  
65

- 845 Sharma T. and Clayton R.N. (1965) Measurement of  $O^{18}/O^{16}$  ratios of total oxygen of carbonates.  
1 846 *Geochimica et Cosmochimica Acta* **29**, 1347-1353.  
2  
3  
4 847 Schmid T. W. and Bernasconi S. M. (2010) An automated method for 'clumped-isotope'  
5  
6 848 measurements on small carbonate samples. *Rapid Communications to Mass Spectrometry*  
7  
8 849 **24**, 1955-1963.  
9  
10 850 Smeraglia L., Bernasconi S.M., Berra F., Billi A., Boschi C., Caracausi A., Carminati E., Castorina F.,  
11  
12 851 Doglioni C., Italiano F., Rizzo A.L., Uysal I.T., Zhao J.-X. (2018) Crustal-scale fluid circulation  
13  
14 852 and co-seismic shallow comb-veining along the longest normal fault of the central Apennines,  
15  
16 853 Italy. *Earth and Planetary Science Letters* **498**, 152-168.  
17  
18 854 Spencer R.J. and Hardie L.A. (1990) Control of seawater composition by mixing of river waters and  
19  
20 855 mid-ocean ridge hydrothermal brines. In: Spencer R.J., Chou I.M. (Eds.), *Fluid Mineral*  
21  
22 856 *Interactions: A tribute to H.P. Eugster. Geochemical Society Special Publication* **2**, 409-419.  
23  
24 857 Stevenson E. I., Rickaby R. E. M., Tyler J. J., Minoletti F., Parkinson I. J., Mokadem F. and Burton K. W.  
25  
26 858 (2014) Controls on stable strontium isotope fractionation in coccolithophores with implications  
27  
28 859 for the marine Sr cycle. *Geochimica et Cosmochimica Acta* **128**, 225–235.  
29  
30 860 Suarez M.B., Ludvigson G.A., González L.A. and You H.-L. (2017) Continental paleotemperatures from  
31  
32 861 an Early Cretaceous dolomitic Lake, Gansu Province, China. *Journal of Sedimentary Research*  
33  
34 862 **87**, 486-499.  
35  
36 863 Van Lith Y., Vasconcelos C., Warthmann R., Martins J. C. F. and McKenzie J. A. (2002) Bacterial sulfate  
37  
38 864 reduction and salinity: Two controls on dolomite precipitation in Lagoa Vermelha and Brejo  
39  
40 865 do Espinho (Brazil). *Hydrobiologia* **485**, 35-49.  
41  
42 866 Vasconcelos C. and McKenzie J.A. (1997) Microbial mediation of modern dolomite precipitation and  
43  
44 867 diagenesis under anoxic conditions (Lagoa Vermelha, Rio de Janeiro, Brazil). *Journal of*  
45  
46 868 *Sedimentary Research, Section A* **67**, 378-390.  
47  
48 869 Vasconcelos C., McKenzie J. A., Warthmann R. and Bernasconi S. M. (2005) Calibration of the  $\delta^{18}O$   
49  
50 870 paleothermometer for dolomite precipitated in microbial cultures and natural environments.  
51  
52 871 *Geology* **33**, 317-320.  
53  
54 872 Warren J. (2000) Dolomite: occurrence, evolution and economically important associations. *Earth-*  
55  
56 873 *Science Reviews* **52**, 1-81.  
57  
58  
59  
60  
61  
62  
63  
64  
65

874 Wilson E.N. Hardie L.A. and Phillips O.M. (1990) Dolomitization front geometry, fluid flow patterns,  
1 875 and the origin of massive dolomite: the Triassic Latemar buildup, Northern Italy. *American*  
2 *Journal of Science* **290**, 741-796.  
3 876  
4  
5  
6 877 Winkelstern I. Z. and Lohmann K. C. (2016) Shallow burial alteration of dolomite and limestone  
7 clumped isotope geochemistry. *Geology* **44**, 463-466.  
8 878  
9  
10 879 Winkelstern I. Z., Kaczmarek S. E., Lohmann K. C. and Humphrey J. D. (2016) Calibration of dolomite  
11 clumped isotope thermometry. *Chemical Geology* **443**, 32-38.  
12 880  
13  
14 881 Wright D.T. (1997) An organogenic origin for widespread dolomite in the Cambrian Eilean Dubh  
15 Formation, northwestern Scotland. *Journal of Sedimentary Research* **67**, 54-64.  
16 882  
17  
18 883 Wright D.T. (1999) The role of sulphate-reducing bacteria and cyanobacteria in dolomite formation in  
19 distal ephemeral lakes of the Coorong region, South Australia. *Sedimentary Geology* **126**,  
20 884 147-157.  
21  
22 885  
23  
24 886 Zheng Y.-F. (1999) Oxygen isotope fractionation in carbonate and sulfate minerals. *Geochemical*  
25 *Journal* **33**, 109-126.  
26 887  
27  
28  
29 888 Zorn H. (1971) Paläontologische, stratigraphische und sedimentologische Untersuchungen des  
30 Salvatoreddolomits (Mitteltrias) der Tessiner Kalkalpen. In: E. Kuhn-Schnyder und B. Peyer, Die  
31 889 Triasfauna der Tessiner Kalkalpen. XXI. *Schweizerische Paläontologische Abhandlungen* **91**, 1-  
32 890 90.  
33  
34 891  
35  
36  
37 892  
38  
39 893  
40  
41  
42  
43  
44  
45  
46  
47  
48  
49  
50  
51  
52  
53  
54  
55  
56  
57  
58  
59  
60  
61  
62  
63  
64  
65

894 Figure Captions:

1  
2 895 Fig. 1. X-ray diffraction pattern of the two natural calibration samples retrieved from the sediments  
3  
4 896 of the Brazilian Lagoa Vermelha. The upper XRD pattern corresponds to sample LV 15 cm and the  
5  
6 897 lower to sample LV 71 cm.  
7

8 898  
9

10  
11 899 Fig. 2. XRD patterns of 'dolomite' samples synthesized under controlled laboratory conditions (Table  
12  
13 900 1); upper pattern 70 °C, 12 weeks; middle pattern 140 °C, 5.6 weeks; and lower pattern 220 °C, 12  
14  
15 901 weeks.  
16

17 902  
18

19 903 Fig. 3. XRD pattern of the ordered stoichiometric dolomites Rodolo (upper green XRD pattern) Sansa  
20  
21 904 (middle XRD pattern) and the international dolomite standard NIST SRM 88b (lower XRD pattern).  
22

23 905  
24

25  
26 906 Fig. 4. The clumped isotope composition of the synthetic and natural dolomite calibration samples  
27  
28 907 digested at 70 °C is plotted against the reciprocal formation temperature. The linear relationship  
29  
30 908 displayed in the top left is derived from the 270 individual replicates of the samples formed at  
31  
32 909 temperatures between 25 and 220 °C. Averages of the 19 different samples are displayed as  
33  
34 910 diamonds with their uncertainty at the 95% CI.  
35

36 911  
37

38 912 Fig. 5. Including the two dolomite samples that were heated to 1100 °C we obtain a third order  
39  
40 913 polynomial  $\Delta_{47}$ -T relationship based on 416 individual measurements covering the full range of  
41  
42 914 potential temperature of dolomite rocks.  
43

44 915  
45

46 916 Fig. 6. The dolomite specific  $\Delta_{47}$ -T calibration of this study is displayed as black line and lies above the  
47  
48 917 calcite specific  $\Delta_{47}$ -T calibration of the ETH (Kele et al., 2015 re-evaluated in Bernasconi et al., 2018)  
49  
50 918 as grey line for 70 °C acid digestion. Both temperature relationships are embedded in 95% CI as  
51  
52 919 dashed lines in the corresponding color.  
53

54 920  
55

56  
57 921 Fig. 7. The new dolomite specific  $\Delta_{47}$ -T calibration was projected to 90 °C acid digestion temperature  
58  
59 922 using the AC of 0.0204 ‰ (Defliese et al., 2015, dashed black line), the AC of 0.0380 ‰ (Murray et  
60  
61 923 al., 2016, black line with dashes and dots) to compare it directly to the dolomite calibration Bonifacie  
62  
63  
64  
65

924 et al., 2017 (grey line in the middle). The top left box shows a blow-up to better visualize the offsets  
1 925 at the temperature range between 70 to 92 °C.  
2  
3

4 926  
5  
6 927 Fig. 8. The black line corresponds to the third order polynomial fit (equation in figure) through all of  
7  
8 928 our dolomite calibration samples between 25 and 1100 °C and the dashed black line corresponds to  
9  
10 929 the theoretical dolomite  $\Delta_{47}$ -T relationship from Guo et al. (2009).  
11

12 930  
13  
14  
15 931 Fig. 9. The oxygen isotope fractionation between (proto-)dolomites and precipitation solutions of the  
16  
17 932 individual synthesized samples of this study (70, 140 and 220 °C, black hollow diamonds), samples of  
18  
19 933 Horita, 2014 (black squares) and of Vasconcelos et al., 2005 (black triangles) are plotted against the  
20  
21 934 inverse temperature. Combination of these three datasets resulted in the black dashed line giving  
22  
23 935 the depicted linear relationship and covers a temperature range from 25 to 350 °C. As dashed grey  
24  
25 936 line we also plotted the one of Matthew and Katz (1977; corrected for the acid digestion factor of  
26  
27 937 Rosenbaum and Sheppard (1986) for consistent data treatment) lying slightly below the combined  
28  
29 938 one.  
30

31 939  
32  
33  
34  
35  
36  
37  
38  
39  
40  
41  
42  
43  
44  
45  
46  
47  
48  
49  
50  
51  
52  
53  
54  
55  
56  
57  
58  
59  
60  
61  
62  
63  
64  
65



Figure 1

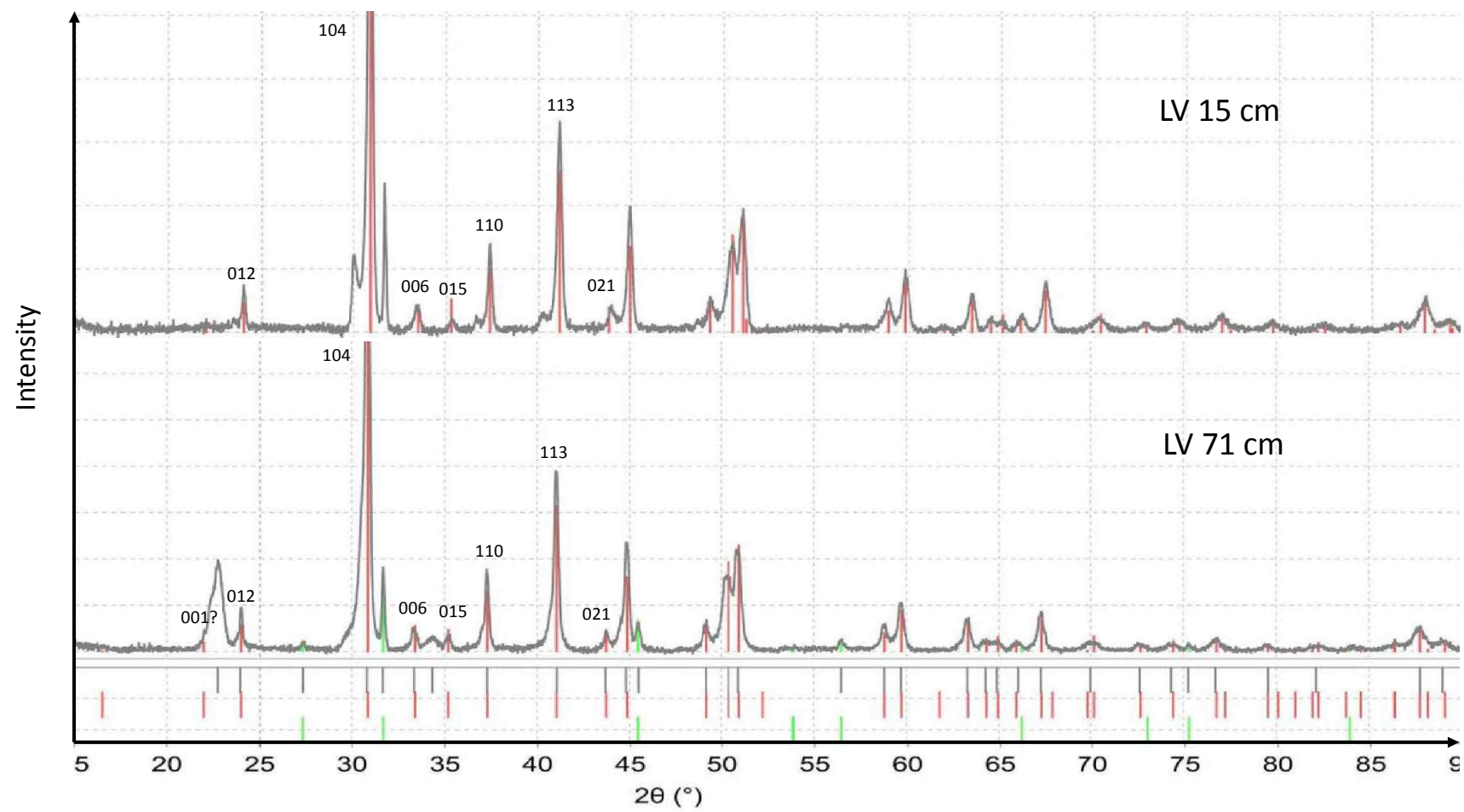


Figure 2

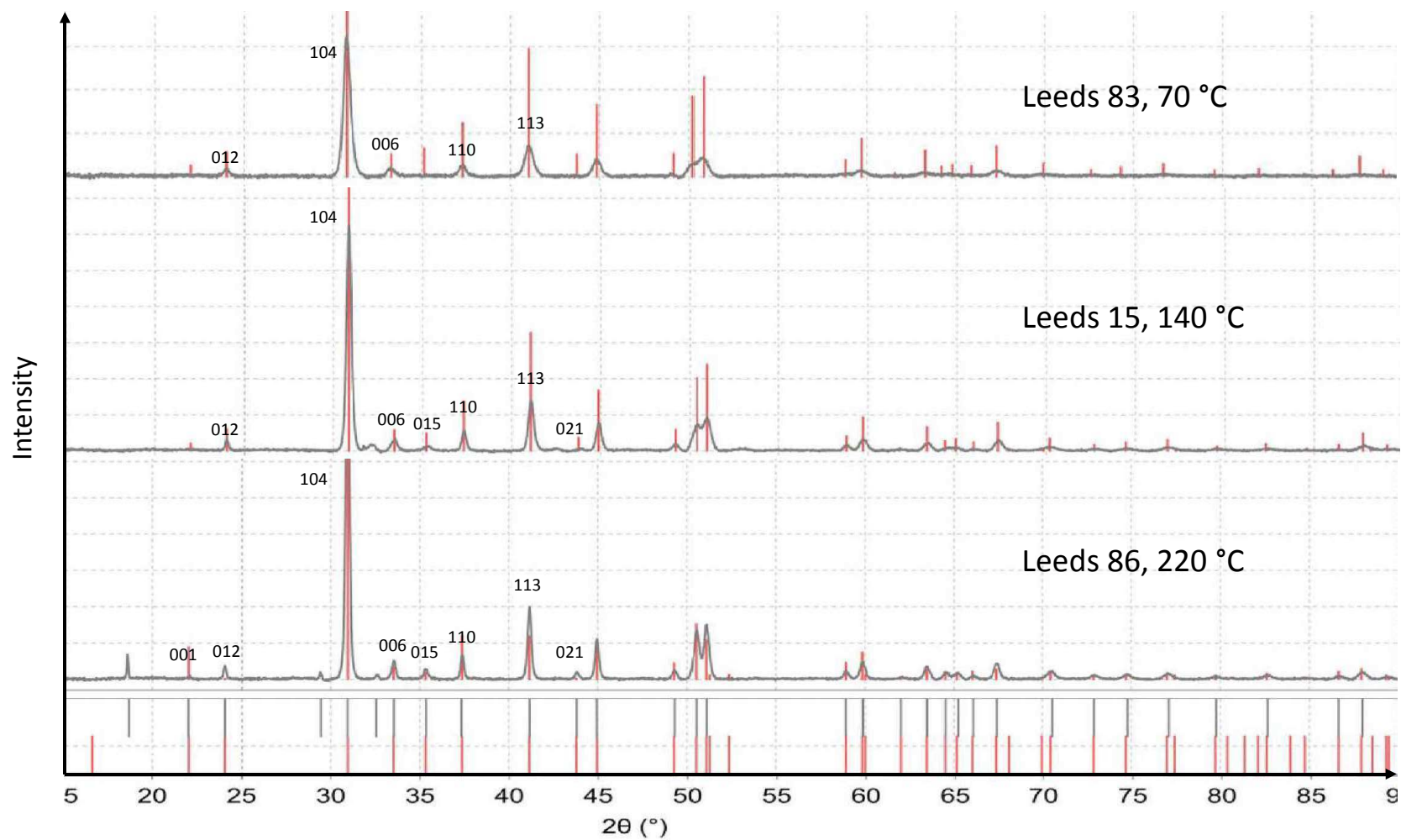


Figure 3

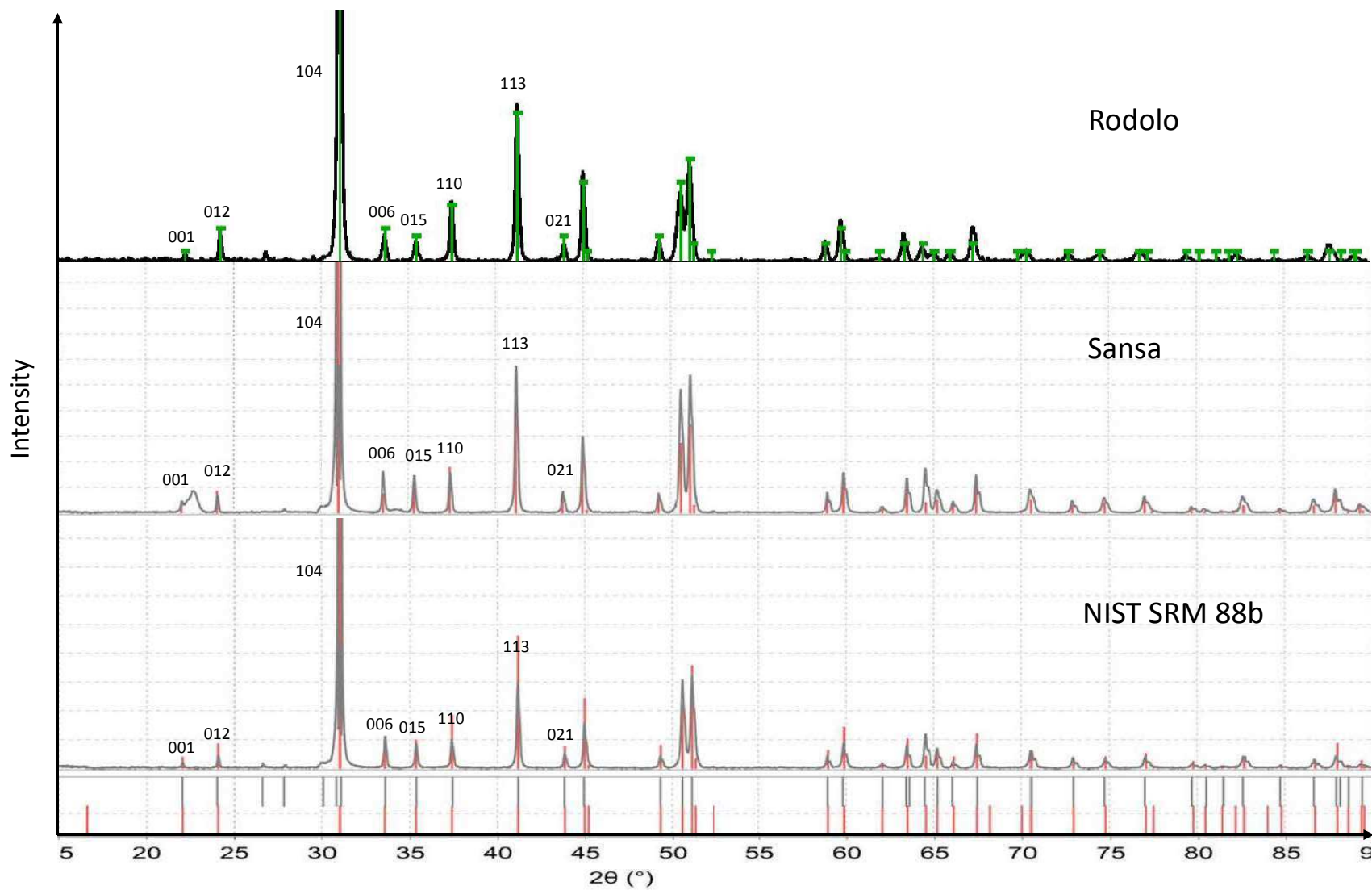


Figure 4

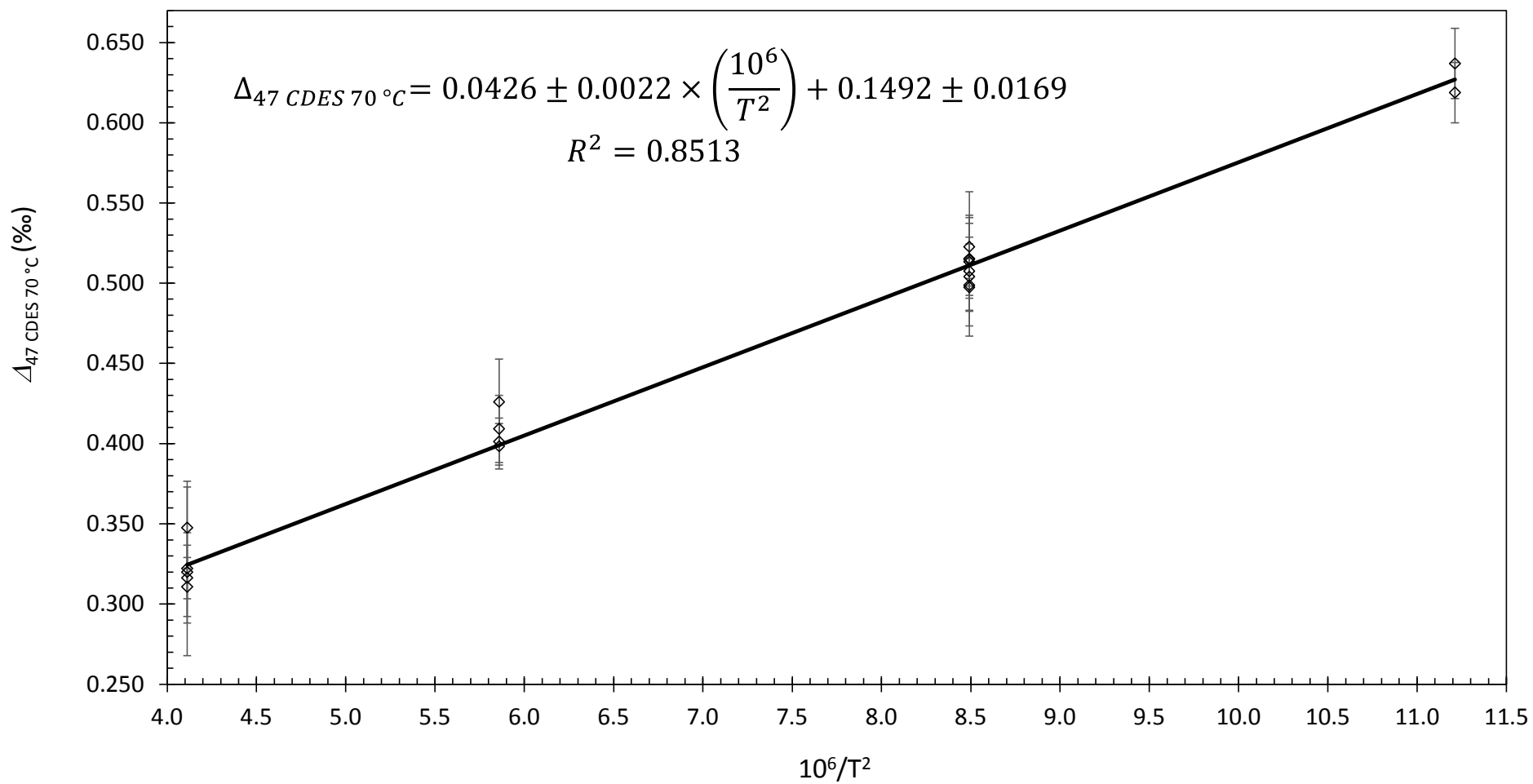


Figure 5

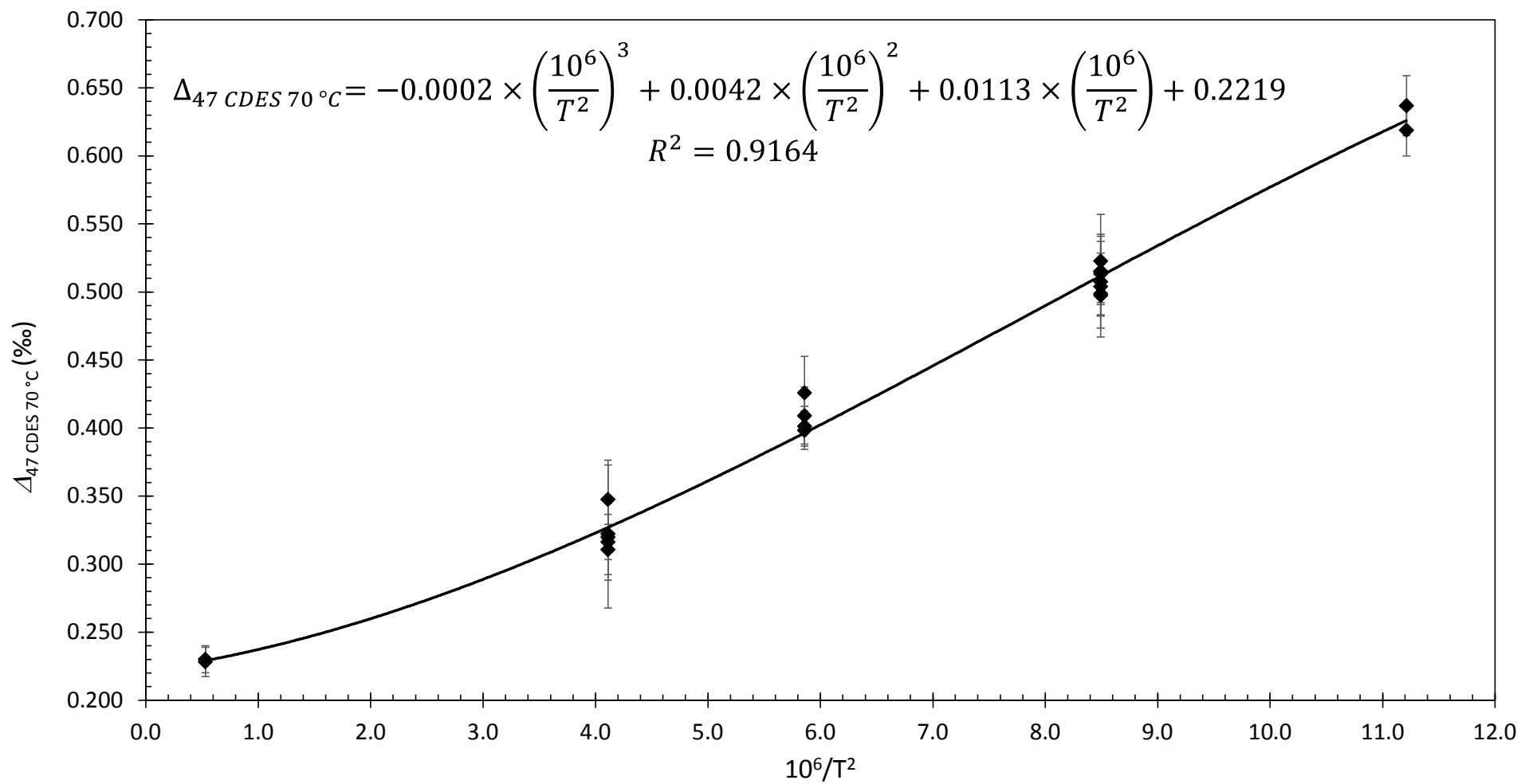


Figure 6

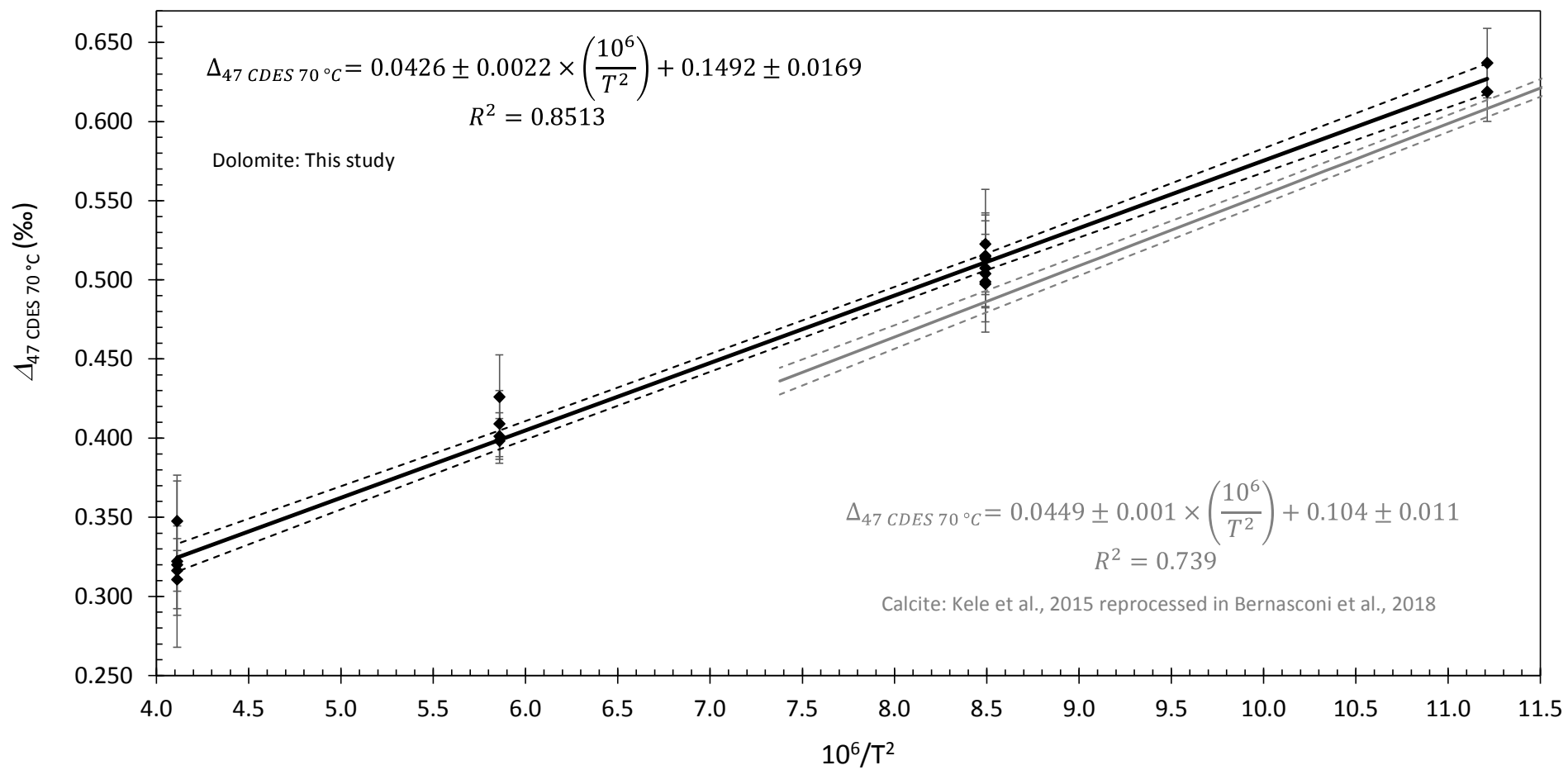


Figure 7

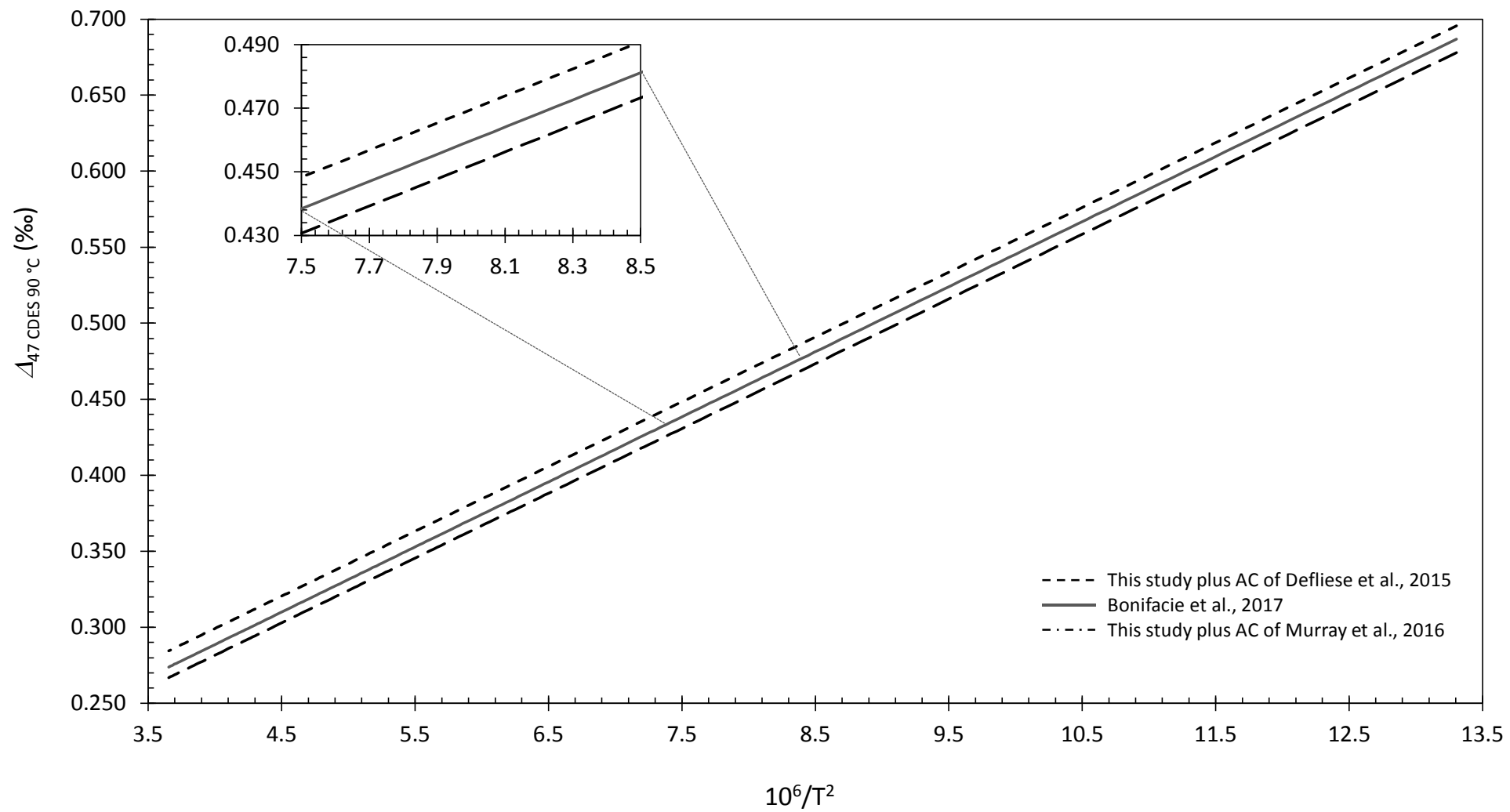


Figure 8

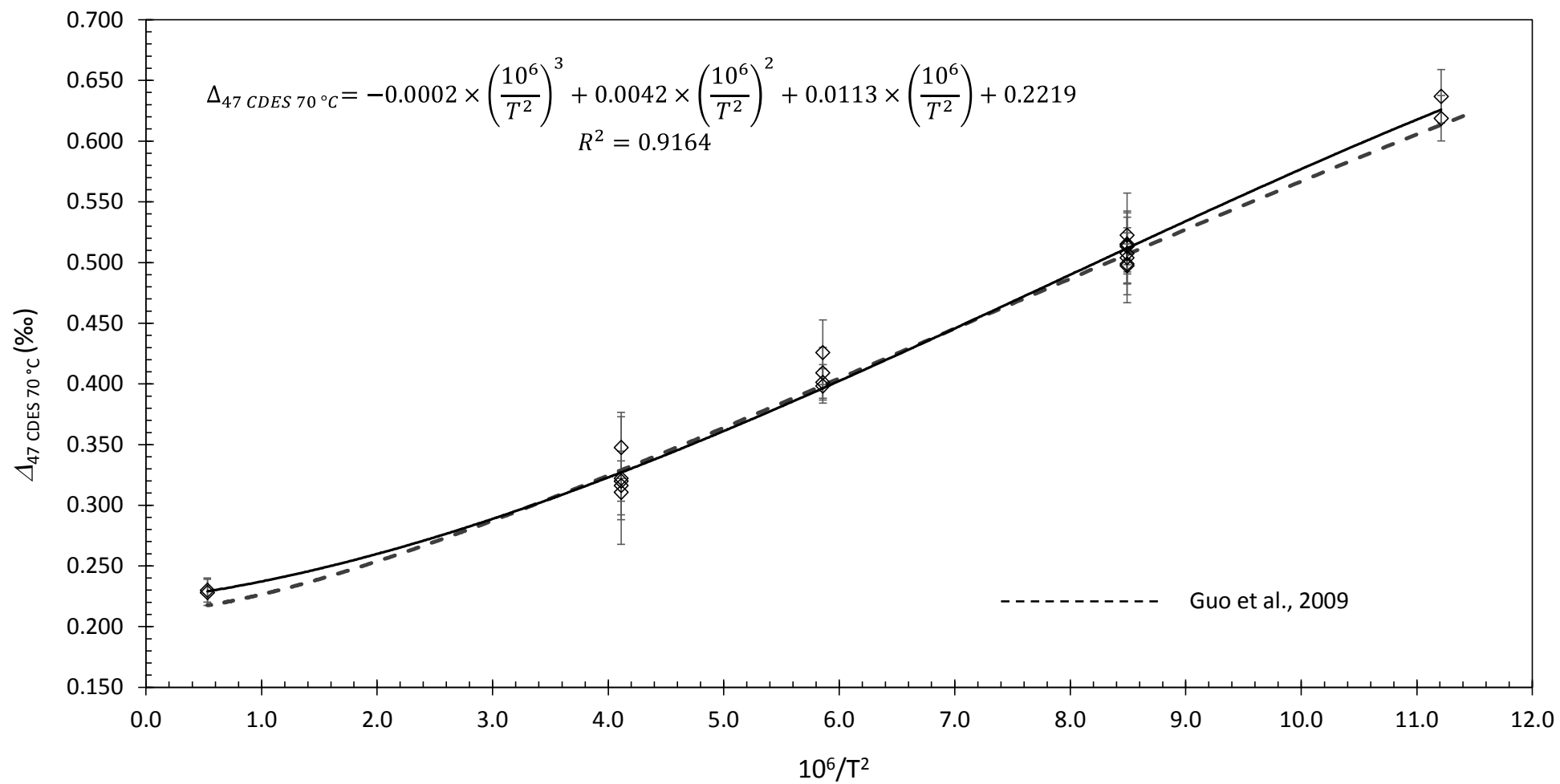
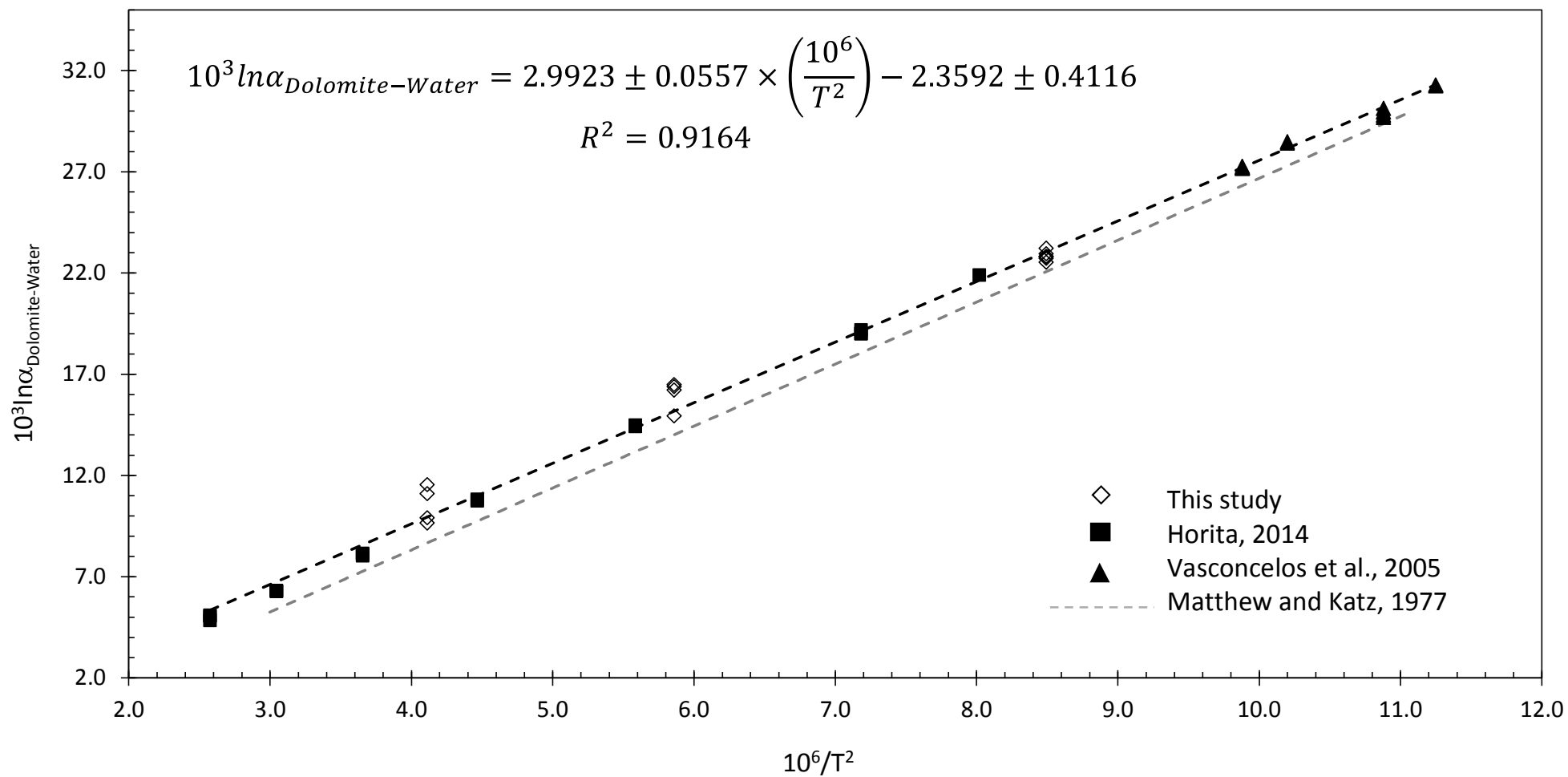




Figure 9



**Table 1**[Click here to download Table: Table 1.docx](#)**Table 1. Oxygen isotope fractionation between Dolomite and Fluid source**

Identifier	T (°C)	Time (weeks)	$\delta^{18}\text{O}_{\text{VSMOW}} (\text{‰})$	$\delta^{18}\text{O}_{\text{H}_2\text{O,VSMOW}} (\text{‰})$	$10^3 \ln \alpha_{\text{Dolomite-Water}}$
LV 15 cm	25.5		34.58±0.05	1.8±1.0	32.19
LV 71 cm	25.5		34.39±0.04	1.8±1.0	32.01
Leeds 23	70	1.0	15.73±0.05	-7.31±0.1	22.95
Leeds 1	70	1.1	15.97±0.11	-7.35±0.1	23.23
Leeds 6	70	1.1	15.53±0.06	-7.36±0.1	22.79
Leeds 12	70	2.4	15.53±0.21	-7.28±0.1	22.72
Leeds 20	70	4.0	15.59±0.05	-7.33±0.1	22.82
Leeds 82	70	12.0	15.98±0.03	-5.99±0.1	21.86
Leeds 83	70	12.0	15.50±0.10	-7.12±0.1	22.53
Leeds 21	140	1.0	7.85±0.20	-7.31±0.1	14.94
Leeds 14	140	2.4	9.38±0.09	-7.13±0.1	16.49
Leeds 22	140	4.0	9.30±0.20	-7.10±0.1	16.39
Leeds 15	140	5.6	9.19±0.07	-7.05±0.1	16.22
Leeds 34	220	2.1	6.14±0.54	-6.91±0.1	13.05
Leeds 41	220	4.0	4.82±0.44	-6.71±0.1	11.54
Leeds 84	220	12.0	4.92±0.23	-4.74±0.1	9.66
Leeds 85	220	12.0	5.19±0.21	-4.72±0.1	9.91
Leeds 86	220	12.0	5.74±0.15	-5.37±0.1	11.10

All uncertainties are displayed at the 95% CL; oxygen isotope composition of the fluid source of samples LV 15 cm and 71 cm are derived from van Lith et al., 2002

**Table 2**[Click here to download Table: Table 2.docx](#)Table 2. Averages of dolomite  $\Delta_{47}$ -T calibration samples

Identifier	T (°C)	$\delta^{33}\text{C}_{\text{VPDB}}$ (‰)	$\delta^{38}\text{O}_{\text{VPDB}}$ (‰)	$\delta^{47}$ (‰)	$\Delta_{47}$ CDES 70 °C (‰)	#
LV 15 cm	25.5	-8.32±0.02	3.56±0.05	10.87±0.08	0.637±0.022	16
LV 71 cm	25.5	-10.21±0.02	3.38±0.04	8.83±0.07	0.619±0.019	16
Leeds 23	70	-7.07±0.03	-14.72±0.05	-6.81±0.12	0.508±0.017	16
Leeds 1	70	-7.10±0.04	-14.51±0.11	-6.70±0.11	0.497±0.014	12
Leeds 6	70	-7.17±0.03	-14.90±0.06	-7.07±0.06	0.523±0.020	11
Leeds 12	70	-7.12±0.09	-14.92±0.21	-7.10±0.26	0.504±0.037	8
Leeds 20	70	-7.22±0.02	-14.86±0.05	-7.13±0.08	0.515±0.042	9
Leeds 81	70	-7.24±0.04	-14.89±0.10	-7.09±0.10	0.515±0.022	18
Leeds 82	70	-7.12±0.02	-14.48±0.03	-6.67±0.07	0.499±0.016	21
Leeds 83	70	-7.25±0.04	-14.94±0.10	-7.15±0.11	0.513±0.015	41
Leeds 21	140	-7.38±0.02	-22.37±0.20	-15.09±0.19	0.426±0.027	6
Leeds 14	140	-7.30±0.03	-20.88±0.09	-13.61±0.18	0.398±0.014	15
Leeds 22	140	-7.35±0.06	-20.96±0.20	-13.74±0.30	0.401±0.015	9
Leeds 15	140	-7.32±0.04	-21.07±0.07	-13.75±0.15	0.409±0.021	21
Leeds 34	220	-7.45±0.14	-24.03±0.54	-16.95±0.70	0.322±0.054	6
Leeds 41	220	-7.45±0.07	-25.31±0.44	-18.43±0.77	0.348±0.025	6
Leeds 84	220	-7.42±0.02	-25.21±0.23	-18.25±0.37	0.311±0.018	12
Leeds 85	220	-7.42±0.02	-24.95±0.21	-17.91±0.30	0.316±0.028	16
Leeds 86	220	-7.31±0.02	-24.42±0.15	-17.31±0.24	0.320±0.017	11
Rodolo (H)	1100	-3.89±0.02	1.78±0.04	13.16±0.05	0.230±0.010	87
Sansa (H)	1100	1.29±0.02	-3.68±0.04	12.54±0.06	0.228±0.011	59

All uncertainties are displayed at the 95% CL

**Table 3**[Click here to download Table: Table 3.docx](#)

Table 3. Dolomite Standards

Identifier	$\delta^{13}\text{C}_{\text{VPDB}}$ (‰)	$\delta^{18}\text{O}_{\text{VPDB}}$ (‰)	$\Delta_{47}^{\text{CDES}, 70^\circ\text{C}}$ (‰)	T (°C)	$\delta^{18}\text{O}_{\text{fluid}}$ (‰)	#
Rodolo	-3.71±0.01	2.77±0.02	0.632±0.006	25±2	1.7±0.4	151
Sansa	1.45±0.04	-3.56±0.09	0.526±0.014	64±6	2.8±1.0	19
NIST SRM 88b	2.12±0.06	-7.09±0.08	0.522±0.022	66±10	-0.5±1.5	14

All uncertainties are displayed at the 95% CI,  $\delta^{18}\text{O}_{\text{fluid}}$  calculated by using combined T relationship of this study

**Table 4**[Click here to download Table: Table 4.docx](#)Table 4. Heated Carbonates ( $\Delta_{47}$  acid fractionations)

Identifier	$\delta^{13}\text{C}_{\text{VPDB}}$ (‰)	$\delta^{18}\text{O}_{\text{VPDB}}$ (‰)	$\Delta_{47}$ CDES 70 °C (‰)	#
<b>Aragonites</b>				
<i>Billin 1 (H)</i>	3.10±0.01	-8.36±0.01	0.165±0.009	64
<i>Billin 2 (H)</i>	-10.99±0.06	-5.59±0.05	0.176±0.013	38
Average			0.169±0.007	102
<b>Calcites</b>				
<i>MS 2 (H)</i>	2.06±0.01	-1.91±0.02	0.183±0.008	88
<i>ETH-4 (H)</i>	-10.20±0.01	-18.72±0.02	0.187±0.008	107
<i>Merck (H)</i>	-41.91±0.02	-15.62±0.01	0.192±0.009	66
Average			0.187±0.005	258
<b>Dolomites</b>				
<i>Rodolo (H)</i>	-3.89±0.02	1.78±0.04	0.229±0.009	91
<i>Sansa (H)</i>	1.29±0.02	-3.68±0.04	0.226±0.010	57
Average			0.227±0.007	148

All uncertainties are displayed at the 95% CL